A semi-Lagrangian water temperature model for advection-dominated river systems

John R. Yearsley[1]

Received 1 December 2008; revised 28 July 2009; accepted 8 September 2009; published 8 December 2009.

[1] This paper describes a one-dimensional stream temperature model that is computationally efficient and highly scalable in both time and space. The model is developed within the framework of state space structure. The time-dependent equations for the conservation of thermal energy in a flowing stream or river are solved using a mixed Eulerian-Lagrangian, or semi-Lagrangian, numerical scheme. Solutions are obtained by tracking individual water parcels along their flow characteristics and storing the simulated results at discrete points on a fixed grid. Computational efficiency and accuracy of the numerical scheme are demonstrated by comparison of model estimates with observations of stream temperatures from rivers in the Pacific Northwest as well as with results from a closed-form solution of the energy equation. A preliminary analysis of the impact of climate changes on stream temperature in the Columbia River system illustrates the strengths of the semi-Lagrangian method for addressing water quality issues of regional, national, and, ultimately, global scale. Further development of the semi-Lagrangian method has the potential to improve the ability of water quality planners to perform uncertainty analysis, risk analysis, and forecasting for large, complex river systems.

Citation: Yearsley, J. R. (2009), A semi-Lagrangian water temperature model for advection-dominated river systems, *Water Resour. Res.*, *45*, W12405, doi:10.1029/2008WR007629.

1. Introduction

[2] Water temperature plays a critical role in the functioning of aquatic ecosystems. It directly influences biota through its control on the flow of energy, metabolic rates of aquatic organisms, and their productivity. The influence of water temperature on aquatic ecosystems occurs over a broad spectrum of space and time scales; and it is therefore important that methods for predicting temperature should be scalable in space and time. A variety of analytical methods have been developed for the analysis of stream temperature and for addressing temperature-related impacts on aquatic ecosystems. These include linear and multiple regression methods [*Mohseni et al.*, 1998; *Donato*, 2002] and neural network models [*Risley et al.*, 2003], both of which make use of existing data to establish relationships between land use and climatic variables and water temperature. These "trainable" data-dependent methods are appealing intuitively and practically because they provide direct relationships between water temperature measurements and state variables. *Donato* [2002], for example, included a wide range of geographical, vegetation, and climate variables in a statistical analysis of water temperature in the Salmon River in Idaho. However, because data-dependent methods are developed from past information, they are limited in their ability to predict future impacts if geographical, vegetation, and climate environmental conditions in a river basin change.

[3] Process models derived empirically from first principles, or a combination of first principles and empirical approaches are more applicable to predicting future impacts. Process models for water temperature based on the First Law of Thermodynamics have been applied in a wide variety of aquatic environments beginning with early applications to the world oceans [*Sverdrup et al.*, 1942]. *Poole and Berman* [2001] provide a qualitative description of many of the natural components comprising the thermal energy balance of streams.

[4] Concerns about the impact of reservoir operations on water temperature and aquatic ecosystems provided motivation for early applications of the thermal energy budget method [*Burt*, 1958; *Delay and Seaders*, 1966; *Raphael*, 1962]. Numerous studies of the thermal discharges from electric power generating facilities were performed using the thermal energy budget method [*Edinger et al.*, 1974] prior to regulation of once-through cooling by the Federal Clean Water Act of 1972 (FWPCA).

[5] More recently, process models based on the thermal energy budget method have been used to develop water quality plans and support management of aquatic resources. Models used for these purposes include SNTEMP [*Theurer et al.*, 1984], HEAT SOURCE [*Boyd and Kasper*, 2003], QUAL2K [*Chapra et al.*, 2008], MASS1 [*Richmond et al.*, 2000], FJQHW97 [*Foreman et al.*, 1997] and CE-QUAL_W2 [*Cole and Wells*, 2002]. The successful application of models of this type demonstrates the value of thermal energy balance method. However, there is need for simulating environmental impacts on aquatic ecosystems at large time and space

[1]Department of Civil Engineering, University of Washington, Seattle, Washington, USA.

Copyright 2009 by the American Geophysical Union.
0043-1397/09/2008WR007629

Table 1. Standard Deviation of Differences Between Simulated and Observed Water Temperature for Various Models Based on the Thermal Energy Budget

River System	River Flow (m^3/s)	Model	Simulation Period[a]	Observed-Simulated Standard Deviation[b] (°C)
Straight R. (Minnesota)	1.0–2.0	MNSTRM [*Sinokrot and Stefan*, 1993]	Days (Hourly)	0.18–0.60
Baptism R. (Minnesota)	1.0–4.1	MNSTRM [*Sinokrot and Stefan*, 1993]	Days (Hourly)	0.79–1.04
Clearwater R. (Minnesota)	0.9	MNSTRM [*Sinokrot and Stefan*, 1993]	Days (Hourly)	0.57
Zumbro R. (Minnesota)	19.4–64.6	MNSTRM [*Sinokrot and Stefan*, 1993]	Days (Hourly)	0.16–0.83
Mississippi R. (Minnesota)	351.3	MNSTRM [*Sinokrot and Stefan*, 1993]	Days (Hourly)	0.47
Santiam R. (Oregon)	28.3–226.5	CE-QUAL-W2 [*Sullivan and Rounds*, 2004]	Months (Hourly)	0.50–1.16
Fraser R. (British Columbia)	1000–7000	FJQHW97 [*Foreman et al.*, 1997]	Months (Daily)	0.72–1.50

[a]Time scale is given in parentheses.
[b]Includes standard deviation, root-mean-square error and standard error of estimate.

scales when addressing issues like climate change [*Intergovernmental Panel on Climate Change* (*IPCC*), 2007]. There is also a need for computationally efficient models that implement data assimilation methods [*Stow and Scavia*, 2009; Vrugt et al. 2006; *Pan and Wood*, 2006] as forecasting tools. Models like SNTEMP, HEAT SOURCE, and QUAL2K are appropriate for water quality planning, but were not developed with computer intensive applications in mind. CE-QUAL-W2 has been used to simulate a number of aquatic ecosystem state variables, including water temperature, in estuaries, lakes, reservoirs and river basin systems. However, CE-QUAL-W2 has limited applicability for large river systems due to complex input data requirements. MASS1 and FJQHW97 have been applied to large river basins like the Columbia and Fraser, but their utility for simulating water temperature at the time scale of decades and continental space scales is not known and, as is the case for CE-QUAL-W2, are limited by the need to satisfy stability criteria of the kind described later in this paper.

[6] In addition to the complexity introduced by larger time and length scales, there has been increasing emphasis on the uncertainty of the output from mathematical models [*Manson and Wallis*, 2000]. Incorporating uncertainty requires a framework in which model outputs are treated as random variables rather than exact estimates of system state. This work addresses the issues of uncertainty in estimating ecosystem state variables by developing the model of water temperature within a state space framework [*Schweppe*, 1973]. The objectives are to (1) emphasize the random nature of the state estimates from mathematical models, (2) construct a nominal solution within the state space framework that can be the basis for future work and (3) demonstrate that the semi-Lagrangian technique is an efficient, accurate numerical method appropriate for obtaining the nominal solution.

[7] For purposes of assessing the adequacy of the model framework as the nominal solution, the paper describes tests in which simulated water temperatures are compared to exact solutions for steady flow as well as to observations from river systems in the Pacific Northwest. The semi-Lagrangian numerical method has been the subject of much research and, therefore, only limited number of model tests with exact solutions is described in this work. The results are compared with two other numerical schemes to provide perspective on performance of the numerical method. The examples drawn from the river systems demonstrate the applicability of the model for water quality planning over a broad spectrum of space and time. Finally, the paper describes an application of the method to assessment of climate change impacts on water temperatures in the Columbia and Snake rivers.

2. State Estimation Methods

[8] While there has been increased recognition of the uncertainty in state estimates from mathematical models, implicit in the widely accepted notion that mathematical models can be calibrated and verified is their deterministic structure. That is, estimates of the key variables, or states, from a calibrated verified model can be treated as being exactly determined by preceding events in time or adjacent events in space rather than as random variables. A deterministic model is one for which there is no uncertainty:

$$\frac{d\mathbf{C}(t)}{dt} = \mathbf{f}[\mathbf{C}(t), \mathbf{u}(t)] \tag{1}$$

where

$\mathbf{C}(t)$ a vector of water quality or ecosystem state variables,
$\mathbf{f}$ completely known nonlinear functions,
$\mathbf{u}(t)$ a vector of completely known inputs,
t time.

[9] However, there is uncertainty in the structure and parameterization of mathematical models as well as uncertainty in the measurement of water temperature. Table 1 provides examples of the uncertainty in the difference between observed and simulated water temperature for a number of thermal energy budget models at various time and space scales. While these examples demonstrate the robust nature of the thermal energy budget method, they also imply the need to incorporate uncertainty into the state estimates.

[10] Mathematical models of water quality with state space structure address the issue of uncertainty by assuming that state estimates are random variables and there is error associated with both the systems model and the measurement model. The equations for propagating the uncertainty of these models are formulated in terms of a process or systems model and a measurement model. The state space continuous form

for a model that treats state variables as random variables is [*Schweppe*, 1973]

$$\frac{d\mathbf{C}(t)}{dt} = \mathbf{f}[\mathbf{C}(t), \mathbf{w}(t), \mathbf{u}(t), t] \tag{2}$$

$$\mathbf{z}(t) = \mathbf{h}[\mathbf{C}(t), \mathbf{v}(t), t] \tag{3}$$

where

h functions mapping the true state to the observations;
w(t) a vector of random input disturbances, (zero mean, covariance $\mathbf{\Psi}$);
z(t) a vector of observations of the state variables;
v(t) a vector of random measurement noise, (zero mean, covariance **R**);

and other variables are as in (1).

[11] The discrete time form of (2) and (3), however, is generally more applicable to the development of ecosystems models:

$$\mathbf{C}(n\Delta + \Delta) = \mathbf{F}[\mathbf{x}(n\Delta), \mathbf{w}(n\Delta), \mathbf{u}(n\Delta), n\Delta)] \tag{4}$$

$$\mathbf{z}(n\Delta) = \mathbf{H}[\mathbf{x}(n\Delta), \mathbf{v}(n\Delta), n\Delta)] \tag{5}$$

where **F**, **H**, **u**, **v**, and **w** are the discrete time counterparts of the continuous time model.

[12] The systems model (4) includes both a deterministic and probabilistic component. The deterministic component is based on the laws of physics, chemistry and biology. Current ecosystems models [*Cole and Wells*, 2002; *Chapra et al.*, 2008] include a wide range of state variables such as water temperature, dissolved oxygen, dissolved nutrients and plant or animal productivity at several trophic levels. This paper considers only water temperature, for which the systems model is based on scientific and empirical knowledge of the thermal energy budget. The probabilistic component, characterized by the vector, **w**, represents the uncertainty in the systems model. Depending on the nature of the problem, the uncertainty can be due to the level of spatial or temporal aggregation, model structure, parameter estimation and input variability.

[13] The measurement model (5) reflects the fact that estimating the water temperature of a system with some form of measuring device, such as a thermistor, cannot be done without uncertainty, characterized in (5) by the vector, **v**. This uncertainty arises from inherent error in the measurement device, sampling error or mapping of point observations to block (areal or volume) predictions.

[14] Linearization techniques [*Schweppe*, 1973] are applied to obtain approximate solutions to (4) and (5) by performing a Taylor expansion of the simplified form of (4),

$$\mathbf{C}(n\Delta + \Delta) = \mathbf{F}[\mathbf{x}(n\Delta), \mathbf{u}(n\Delta), n\Delta] + \mathbf{G}[\mathbf{x}(n\Delta), n\Delta]\mathbf{w}(n\Delta) \tag{6}$$

about a nominal solution,

$$\mathbf{C_{nom}}(n\Delta + \Delta) = \mathbf{F}[\mathbf{x_{nom}}(n\Delta), \mathbf{u}(n\Delta), n\Delta)] \tag{7}$$

[15] Assuming the model uncertainty, **w**, is Gaussian, and neglecting higher order terms, the resulting linearized equations for the propagation of the system state, $\mathbf{C_{nom}}$ and its uncertainty, $\mathbf{\Gamma}$ can be written

$$\mathbf{C_{nom}}(n\Delta + \Delta) = \mathbf{F}[\mathbf{x_{nom}}(n\Delta), \mathbf{u}(n\Delta), n\Delta] \tag{8}$$

$$\mathbf{\Gamma}(\Delta n + \Delta) = \mathbf{F^{(1)}}[\mathbf{x_{nom}}(n\Delta)]\mathbf{\Gamma}(n\Delta)\mathbf{F^{(1)T}}[\mathbf{x}_{nom}(n\Delta)] + \mathbf{G}[\mathbf{x_{nom}}(n\Delta)]\mathbf{Q}\mathbf{G^T}[\mathbf{x}_{nom}(n\Delta)] \tag{9}$$

where

$$\mathbf{F^{(1)}}[\mathbf{C_{nom}}(n\Delta)] = \frac{\partial \mathbf{F}(\mathbf{C})}{\partial \mathbf{C}}|_{\mathbf{C}=\mathbf{C_{nom}}}$$

and

$$E\left[\mathbf{w}(n_1\Delta)\mathbf{w^T}(n_2\Delta)\right] = \begin{cases} \Psi, & \nu_1 = \nu_2 \\ 0, & n_1 \neq n_2 \end{cases}$$

[16] A first step in obtaining solutions of (8) and (9) for water temperature in river systems is to develop the nominal solution, $\mathbf{C_{nom}}$. A key assumption being that the difference between the nominal state and the true system state is small. When water temperature is the state variable, the energy budget method provides a well-tested paradigm for obtaining the nominal solution. With the energy budget as the deterministic input, nominal solutions to (8) can be obtained using numerical methods. The governing hydrodynamic equations can be formulated in an Eulerian frame of reference, in which the reference system is fixed in space and through which the water flows; or a Lagrangian frame of reference in which the reference system moves with the fluid; or a combination of Eulerian and Lagrangian (semi-Lagrangian) reference frames as described below.

[17] Systems models using the Eulerian framework are developed with either finite difference [*Brown and Barnwell*, 1987; *Chapra et al.*, 2008; *Cole and Wells*, 2002; *Foreman et al.*, 1997] or finite element methods [*King*, 1996a, 1996b]. However, finite difference or finite element techniques using the Eulerian framework are subject to accuracy and stability problems [e.g., *Roache*, 1976]. Numerical dispersion, associated with simulating phenomena with sharp concentration gradients can result in undesirable oscillations or spurious damping of high frequencies of state variables. Results can be improved by reducing the numerical grid size, but there is an associated cost in computational efficiency due to the need to also reduce the time step. The stability of many current models with an Eulerian framework is limited by the size of the time step for streams and rivers dominated by advection.

[18] Solution techniques based on the Lagrangian point of view [*Jobson*, 1981] avoid many of the stability and accuracy problems associated with Eulerian methods but lack the computational convenience of a fixed grid. However, hybrid Eulerian-Lagrangian (semi-Lagrangian) methods are efficient, accurate solution methods that combine some of the virtues of each point of view [*Cheng et al.*, 1984; *Yeh*, 1990; *Zhang et al.*, 1993; *Manson and Wallis*, 2000; *Manson et al.*, 2001]. In semi-Lagrangian methods, advective processes are solved in a two-step process. Solutions are obtained by tracking individual water parcels

along their flow characteristics and storing the simulated results at discrete points on a fixed grid. Semi-Lagrangian methods implementing single-step reverse particle tracking (SRPT) are subject to numerical dispersion in the Eulerian step [*Zhang et al.*, 1993]. This is a result of interpolating the initial water parcel conditions on the fixed Eulerian grid. However, studies have shown that semi-Lagrangian methods perform well when compared with Eulerian schemes. *Yeh* [1990] found that the use of hybrid methods with single-step reverse particle tracking (SRPT) was clearly superior to the Eulerian method using what is termed an upwind method. *Zhang et al.* [1993] found that hybrid methods using SRPT introduced some numerical dispersion, but that it could be controlled using a modified form of SRPT. *Cheng et al.* [1984] reported that when linear interpolation was used with hybrid solution techniques, numerical dispersion was similar to that of upwind methods, but were able to eliminate numerical dispersion by using second-order Lagrangian polynomial interpolation.

[19] Semi-Lagrangian methods have considerable appeal because, as *Manson et al.* [2001] point out, they are stable and accurate at large time steps in numerical solutions of fluid transport when advection dominates. They are also highly scalable in both time and space. As a result, they have found acceptance in numerical models for weather forecasting [e.g., *European Centre for Medium-Range Weather Forecasts*, 2006] and large-scale climate models like the National Center for Atmospheric Research (NCAR) model, CAM [*Collins et al.*, 2004]. Applications of the method in water quality simulations are less well known, in spite of the fact it is particularly well suited for applications to large-scale riverine environments where advection dominates. This may be because the space-time scales of water quality planning have generally been at the basin or sub basin level and more attention has been given to the development of water quality parameters rather than to numerical methods.

3. Application of Semi-Lagrangian Methods to Riverine Environments

[20] In the Lagrangian frame of reference the deterministic model for water temperature, T_{nom}, in a one-dimensional system has the form [*Jobson and Schoellhamer*, 1993]

$$\rho C_p \frac{\partial (T_{nom} A_x)}{\partial t} = \partial C_p \frac{\partial}{\partial \xi}\left(\mathrm{K}_L A_x \frac{\partial T_{nom}}{\partial \xi}\right) + S + \frac{\rho C_p Q_{trb} T_{trb}}{D} \tag{10}$$

where

ρ the density of water, kg/m^3;
C_p the specific heat capacity of water, J/kg/°C;
A_x the cross-sectional area of the stream or river channel, m$^{2;}$
K_L the longitudinal dispersion coefficient, m^2/s;
S a source term, J/m/s;
Q_{trb} advected flow from tributaries or groundwater, m^3/s;
T_{trb} advected temperature from tributaries or groundwater, °C;

and ξ is the Lagrangian coordinate given by

$$\xi = x - x_0 - \int_{t_0}^{t} u \, dt' \tag{11}$$

for which x is fixed in space (an Eulerian coordinate), x_0 is the position of the parcel at time, t_0 and u is the cross-sectionally averaged speed. The advection term associated with (10) is of the order O(u/L), where L is a characteristic length and the dispersion term is of order O(K_L/L^2). Advection dominates in a water body when $u/L > K_L/L^2$. *Toprak and Savci* [2007] modeled dispersion coefficients in natural channels and found values varying from 2 m^2/s to 1486 m^2/s with an average of 120 m^2/s. For the average value found by *Toprak and Savci* [2007], stream speeds of the order of 1 m/s, and temperature differences of order 1°C, advection begins to dominate at length scales greater than 100 m. Based on this scaling, the dispersion term is neglected in many studies of natural river systems [e.g., *Foreman et al.*, 2001] and (10) reduces to

$$\rho C_p \frac{d(T_{nom} A_x)}{dt} = S + \frac{\rho C_p Q_{trb} T_{trb}}{D} \tag{12}$$

[21] For the semi-Lagrangian treatment of (12), water temperature is followed along characteristics described by (11) and results are output at discrete points described by the (Eulerian) finite difference grid. In the Lagrangian step, river speed as a function of longitudinal distance during a time period determines the location of a particle of water by single-step reverse particle tracking. The river system is divided into N segments, not necessarily of the same spatial dimensions. Within each segment, however, the speed and geometric properties of the river system are assumed to be constant during a given time step. Water temperature values are recorded only on the boundaries between segments. At the end of a computational time step, $t = n\Delta + \Delta$,), a parcel of water with finite cross-sectional area at the downstream end of a segment, j, is flagged. The flagged parcel is tracked backward in time upstream along its characteristic path using (11) until its position at the beginning of the time step, $t = n\Delta$), is located. The location of a particle tracked in this manner will, in general, not be precisely on a segment boundary where water temperatures are stored by the computational scheme The trajectory of the particle that ended at x_j during the time from $t = n\Delta$ to $t = (n\Delta + \Delta)$) is given by

$$x_j = x_{j0} + \sum_{j'=j0}^{j} u(j')\Delta(j') \tag{13}$$

where

x_{j0} the location of particle x_j at time $t = n\Delta$;
u(j$'$) the speed of the particle in the j'th segment;
$\Delta(j')$ the time it takes to transit the j'th segment, and
$\Sigma\ \Delta$(j$'$) = Δ.

[22] During the time the particle transits the j'th segment the temperature is updated using the discrete time form of the systems model for water temperature. The change in temperature $T_{nom}(n\Delta + \Sigma\Delta(j'))$ of a parcel that ends at the downstream boundary of the j'th segment at time $t = (n\Delta + \Sigma\Delta(j')$ in discrete form is given by

$$\rho C_p [T_{nom}(n\Delta + \Sigma\Delta(j')) - T_{nom}(n\Delta + \Sigma\Delta(j'-1))] = \left[\frac{H_{air-water}(n\Delta, x_{j'})}{D(n\Delta, x_{j'})} + \frac{\rho C_p Q_{trb}(n\Delta, x_{j'}) T_{trb}(n\Delta, x_{j'})}{D(n\Delta, x_{j'})}\right]\Delta(j') \tag{14}$$

Table 2. Properties of the Analytical Solution Used in Model Tests

		Courant Number, $N_{cr} = \Delta tQ/\Delta V$		
Test Case	Residence Time	Semi-Lagrangian	QUAL2E	QUICK
1	2.0	0.50(RBM10i)	0.50	0.0625
1	1.0	1.00(RBM10ii)	-	-
2	1.0	1.00	1.00	0.125
3	0.6	1.67	1.67	0.208
4	0.5	2.00	2.00	0.250

where D is the average water depth in a cross section of the channel and all other terms are as described previously, S, the source term in (12) has been replaced by $H_{air\text{-}watert}(n\Delta, x'_j)$, the exchange of energy across the air-water interface at time $t = n\Delta$, and location, x_j. Exchange of energy across the air-water interface, as shown in the examples that follow (sections 4.2 and 4.3) captures the important features of temperature change in rivers dominated by advection and for which hyporheic flow, riparian vegetation or streambed heat exchange are not important. However, as *Poole and Berman* [2001] discuss, it is important to consider all mechanisms and influences on water temperature when developing the components of the energy source term, S. Hyporheic flow [*Burkholder et al.*, 2008], vegetative shading or topographical shading [*Sridhar et al.*, 2004], and streambed heat exchange [*Sinokrot and Stefan*, 1993], though not considered here, can be included in (14).

[23] The water temperature $T_{nom}(n\Delta)$ of the particle at the beginning of the time step is determined in the Eulerian step by interpolating between the segment boundaries where water temperatures are recorded. In the solution technique used in this study, this is accomplished with a third-order polynomial [*Press et al.*, 1986]. Once the location of the particle and its initial water temperature are determined for the beginning of the time step, the particle is followed back downstream to its location at the end of the time step (the downstream end of segment j). The change in water temperature for the particle during this time step can be estimated using (14) when the speed of the particle, water depth, net exchange across the air-water interface (energy budget) and advected heat sources (tributary input) are known.

[24] The speed of the particle, u, and the depth of water, D, during the time period can be determined in many ways. Since the water temperature model assumes that the water body is well mixed vertically and laterally, density effects due to temperature gradients are neglected. This means that the temperature model can be uncoupled from the model that simulates flow velocity and water depth. The flow velocity and depth can then be determined independently, either by simulation with a hydrodynamic model that solves, numerically, some form of the equations of conservation and mass or a model that uses empirical methods. HEC-RAS [*Hydrologic Engineering Center*, 2002], CEQUAL-W2 [*Cole and Wells*, 2002] and RMA-10 [*King*, 1996a, 1996b] are examples of hydrodynamic models used for simulations of water temperature. When observed flows are available [e.g., *Sinokrot and Stefan*, 1993], the depth, D, and speed, u. can be estimated using relationships of the form [*Chapra*, 1997; *Leopold and Maddock*, 1953]

$$D = aQ^b \tag{15}$$

$$u = cQ^d \tag{16}$$

where a, b, c, and d are empirical constants determined from stage discharge rating curves.

[25] The net exchange of thermal energy, $H_{air\text{-}water}$, across the air-water interface is determined using the methods of *Wunderlich and Gras* [1967]:

$$H_{air-water} = (H_{sw} - H_{rs}) + (H_a - H_{ar}) + H_{evap} + H_{cond} + H_{back} \tag{17}$$

where

$H_{air\text{-}watert}$ net exchange of thermal energy across the air-water interface, J/s/m^2;
H_{sw} shortwave solar radiation, J/s/m^2;
H_{rs} reflected shortwave solar radiation, J/s/m^2;
H_a long wave atmospheric radiation, J/s/m^2;
H_{ar} reflected atmospheric radiation, J/s/m^2;
H_{evap} evaporative heat flux, J/s/m^2;
H_{cond} conductive heat flux, J/s/m^2;
H_{back} blackbody radiation from the water surface, J/s/m^2.

The thermal energy budget terms in (17) can be computed using meteorological data, including barometric pressure, cloud cover, wind speed, air temperature and relative humidity.

4. Model Testing and Application

[27] The numerical method described above was tested by comparing simulated results with known analytical solutions characterized by sharp concentration gradients (short wavelengths) and with observed data from two river systems in the Pacific Northwest. To demonstrate applications to large-scale questions of freshwater habitat, the semi-Lagrangian method was used in a preliminary analysis of the impact of climate change on water temperatures in a major river basin, the Columbia.

4.1. Analytical Solutions

[28] The response of the interpolation scheme used in the semi-Lagrangian numerical method was assessed by comparing results with exact solutions of (10). The exact solution in these example is one for which the concentration of the ideal river system is equal to zero everywhere initially. At time, $t = 0$, at the upstream boundary, ($x = 0$), the concentration is increased by a step function. The resulting analytical function is translated downstream without dispersion. The two Eulerian methods used for comparison in the examples were the fully implicit method and an explicit method, QUICK. QUICK is an upwind biased quadratic interpolation scheme introduced by *Leonard* [1979]. The fully implicit method is the numerical scheme used in QUAL2E and QUAL2K. QUICK represented an important development in numerical methods for solving steady state advection problems and forms the basis for more accurate numerical methods, QUICKEST and ULTIMATE QUICKEST [*Leonard*, 1991].

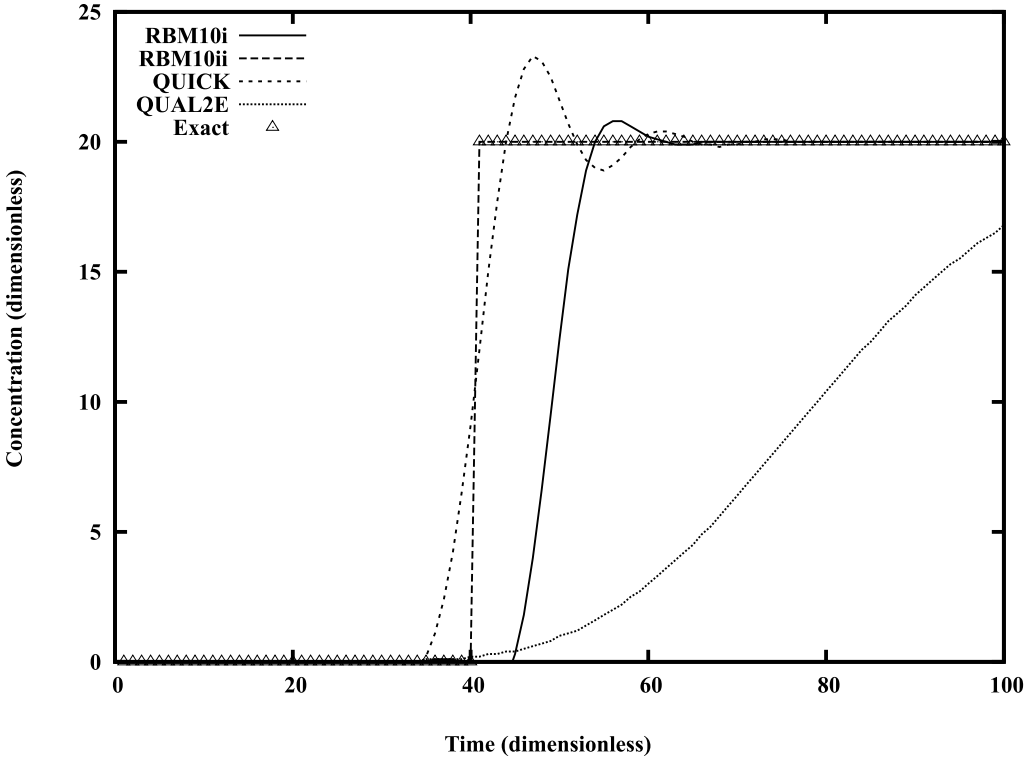

Figure 1. Semi-Lagrangian (RBM10), QUICK, and fully implicit numerical schemes compared to exact solution for step function initial values and computational segment residence time, T_{res} = 2.0.

[29] In these examples, an idealized river system of constant cross section and steady flow was divided into 200 segments of equal length. The boundary condition for the simulated "concentration," C, at the upstream (headwaters) segment was assumed to be of the form

$$C(t, x = 0) = 20u_{-1}(t) \tag{18}$$

where

$$u_{-1}(t) = \begin{cases} = 1, & t \geq 0 \\ = 0, & t < 0 \end{cases}$$

Values of the flow, Q and segment volume, ΔV, for propagation of the step function were chosen such that the computational cell residence time, $T_{res.}$ where

$$T_{res} = \frac{\Delta V}{Q} \tag{19}$$

varied from 0.5 to 2.0 time units (Table 2). The computational time step, Δt, used for both the semi-Lagrangian and full-implicit method was, in all cases, equal to one. For the QUICK method, the computational time step was 0.125 (1/8) time units in all cases so as to satisfy the Courant condition:

$$\Delta t \leq \frac{\Delta V}{Q} \tag{20}$$

The results for the three methods are compared to the true solution in Figures 1–4.

[30] For those examples in which the residence time is an integer, as is the case in Figures 2 and 4, the semi-Lagrangian method gives the same result as the exact solution. This is because the particle trajectory reaches the segment boundary after a time step and there is no "dispersion" associated with the interpolation of water temperatures between segment boundaries in the Eulerian step. In those cases for which the residence time is not an integer, there is also numerical dispersion as well as an initial oscillation associated with the semi-Lagrangian method, although both phenomena are less pronounced than for the other two schemes (Figures 1 and 3).

[31] For the case in which the residence time is less than one (Figure 1), the semi-Lagrangian method shows both numerical dispersion and a phase delay (RBM10i) when the Eulerian grid it uses for interpolation is greater than the distance a water parcel moves in one time step. The phase change is eliminated by choosing the size of the grid such that it is equal to or less than the distance a water parcel moves in one time step (RBM10ii in Figure 1) for the semi-Lagrangian method. For the simulation labeled RBM10ii, the length of each segment was halved, giving the expected result in which the semi-Lagrangian method reproduces the true solution. Simulations with the semi-Lagrangian method for residence times less than one, but not an integer, produce results similar to that of Figure 3 so long as the length of each Eulerian segment is less than the distance a water parcel moves in one time step.

4.2. Clearwater River, Idaho

[32] The Clearwater River in North Central Idaho (Figure 5) flows from the Idaho-Montana border westward,

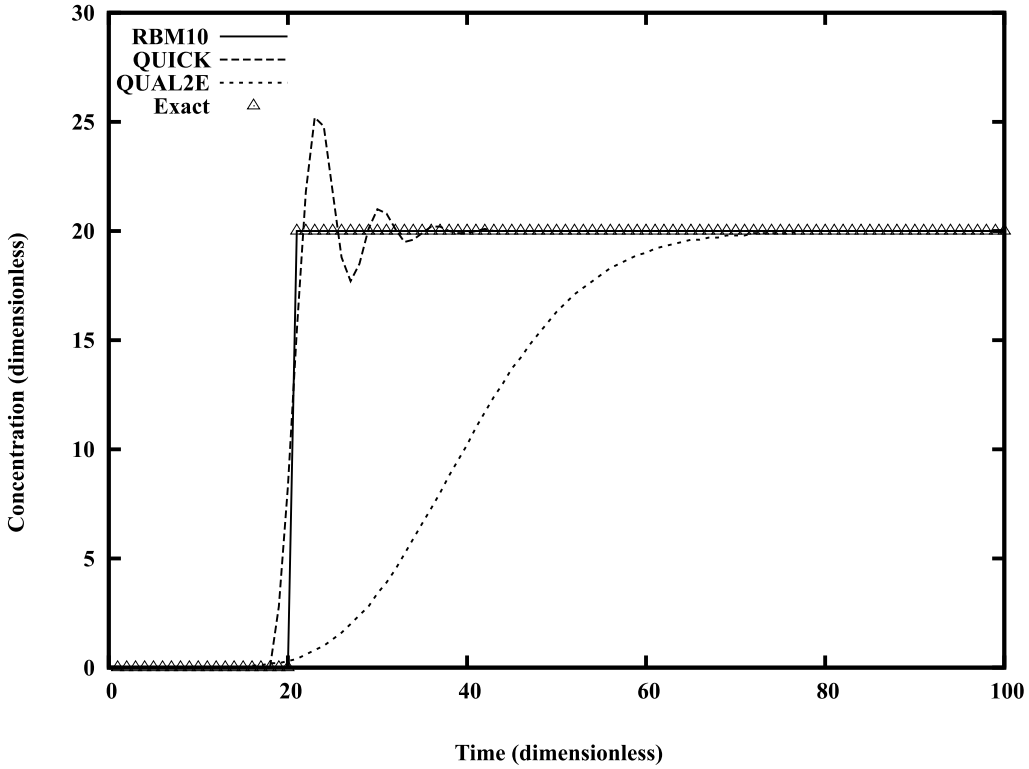

Figure 2. Semi-Lagrangian (RBM10), QUICK, and fully implicit numerical schemes compared to exact solution for step function initial values and computational segment residence time, T_{res} = 1.0.

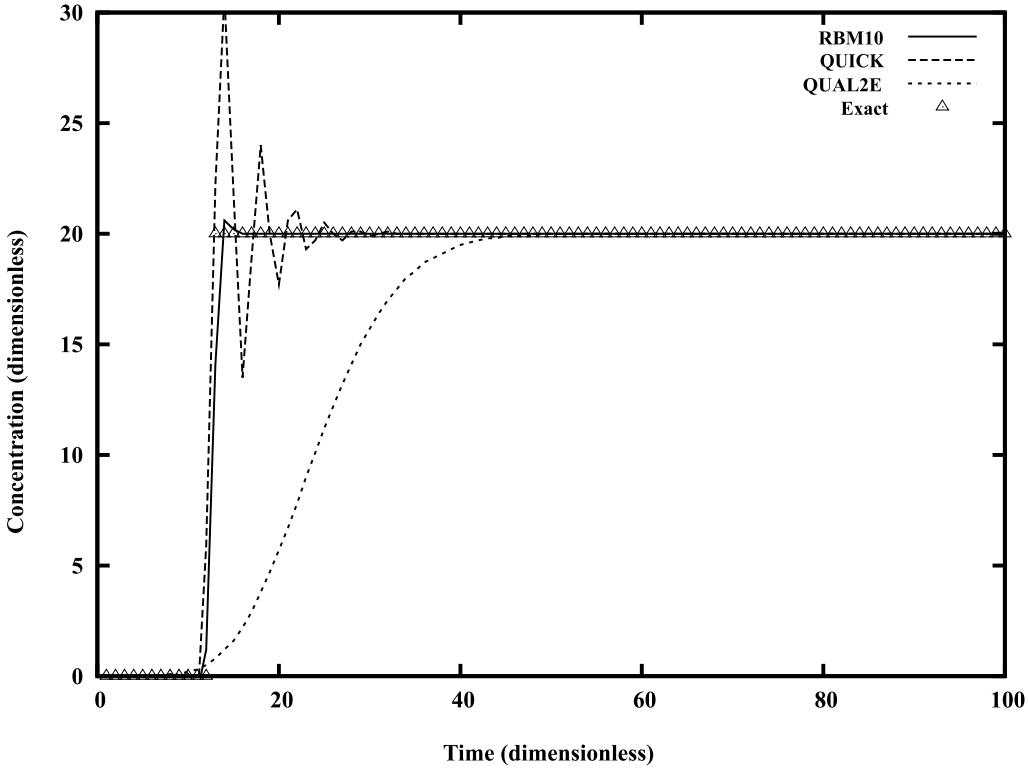

Figure 3. Semi-Lagrangian (RBM10), QUICK, and fully implicit numerical schemes compared to exact solution for step function initial conditions and computational segment residence time, T_{res} = 0.6.

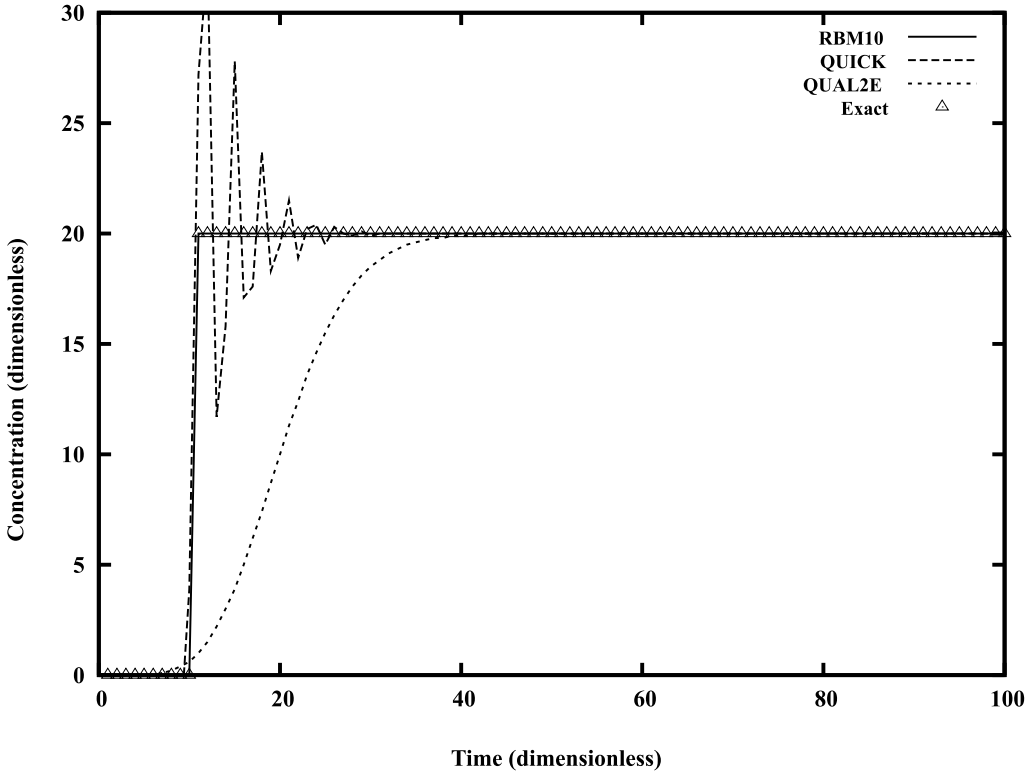

Figure 4. Semi-Lagrangian (RBM10), QUICK, and fully implicit numerical schemes compared to exact solution for step function initial values and computational segment residence time, T_{res} = 0.5.

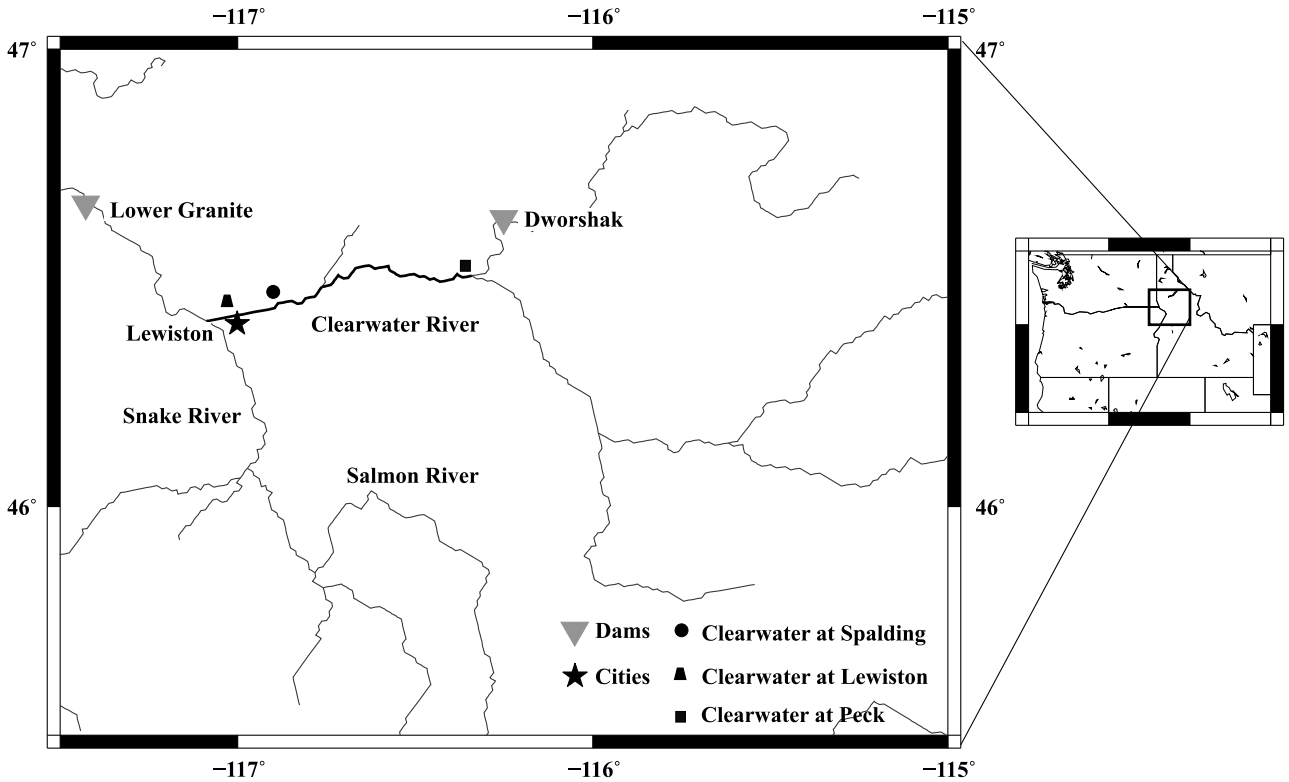

Figure 5. Clearwater River in Idaho.

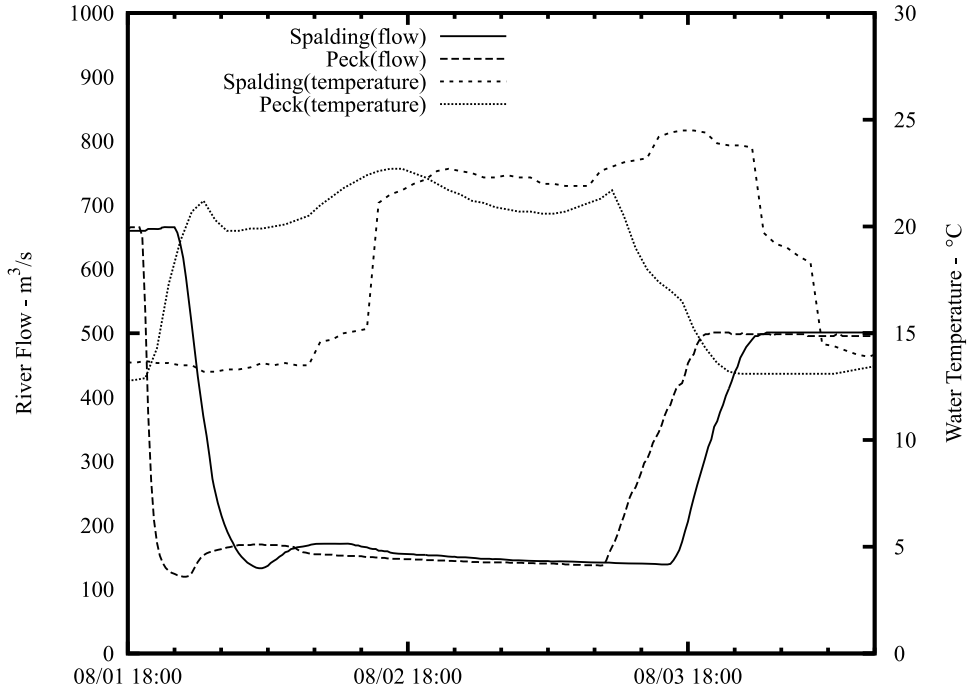

Figure 6. Observed flow and water temperature in the Clearwater River at Peck and Spalding, Idaho, August 1998.

joining the Snake River at Lewiston, Idaho. The Clearwater is the largest tributary of the Snake River, with a drainage area of 24,800 km^2 and a mean annual discharge of 420 m^3/s. Water temperatures in the North Fork Clearwater River and the main stem Clearwater River below the confluence have been altered from natural conditions by releases from Dworshak Dam and Reservoir. Changes from the historic water temperature regime began in 1972 when Dworshak Dam was completed and the North Fork of the Clearwater River behind the dam was impounded.

[33] Dworshak Dam is equipped with multilevel selector gates that are adjustable for selective withdrawal between full pool (488 m mean sea level (msl)) and minimum pool (440 m msl). Since 1992, releases from Dworshak Dam have provided flow augmentation to the Snake River for the benefit of migrating juvenile salmon and steelhead from April through August. More recently, selective withdrawal of water from Dworshak Dam, using the multilevel selector gates, has provided cold water during the late summer to promote the migration of returning adult Chinook salmon.

[34] The operation of Dworshak Dam in this manner results, at times, in significant changes in the flow and water temperature regimes of the Clearwater River. Observations of flow and water temperature at hourly intervals have been made at key locations in the Clearwater (Figure 5). The observations provide valuable data for assessing how well the methods described here are able to simulate water temperatures when there are sharp fronts associated with rapid changes in flow and temperature.

[35] The data required for simulating water temperatures were obtained from several sources. As part of a program to better manage the water resources of the Clearwater River and its tributaries, the U.S. Army Corps of Engineers (USACE) and U.S. Geological Survey (USGS) have established a monitoring program that includes observations of streamflow and water temperature. Meteorological data required for estimating the thermal energy budget are measured at Dworshak Dam by the U.S. Bureau of Reclamation (AGRIMET) and at Lewiston, Idaho by the National Weather Service. The results of dam operations during the months of July and August, 1998 were used as the test case. On August 1, 1998 the flow at Dworshak Dam was decreased from 555.0 m^3/s to 39.65 m^3/s over a period of a few hours and then increased from 39.65 m^3/s to 396.5 m^3/s on August 3 over a similar period of time. The changes in flow and temperature during this period at Peck, Idaho and Spalding, Idaho are shown in Figure 6. The sharp concentration gradients associated with the abrupt changes in flow and temperatures suggest that the dispersion term in (10) may become important at some point. However, the time scale associated with dispersion in this case is such that the shapes of the thermal wave and the hydrodynamic wave have not changed significantly between the observations near Dworshak Dam and the observations at Spalding, Idaho. As a result, it is reasonable to assume that dispersion of the front can be neglected in simulating the water temperature.

[36] Velocity and depth as function of flow at river cross sections were simulated with the steady flow model HEC-RAS [*Hydrologic Engineering Center*, 2002]. The use of HEC-RAS in this case seemed reasonable given that the speed of the gravity wave was such (Figure 6) that the river reached equilibrium within a few hours. In addition, the speed of the gravity wave is greater than that of temperature front and it is the speed of the temperature front that determines the trajectory of the water parcels.

[37] The water temperatures simulated using the semi-Lagrangian method are compared to observed daily averaged and hourly temperatures from temperature monitoring devices at Lewiston, Idaho and Spalding, Idaho as shown in

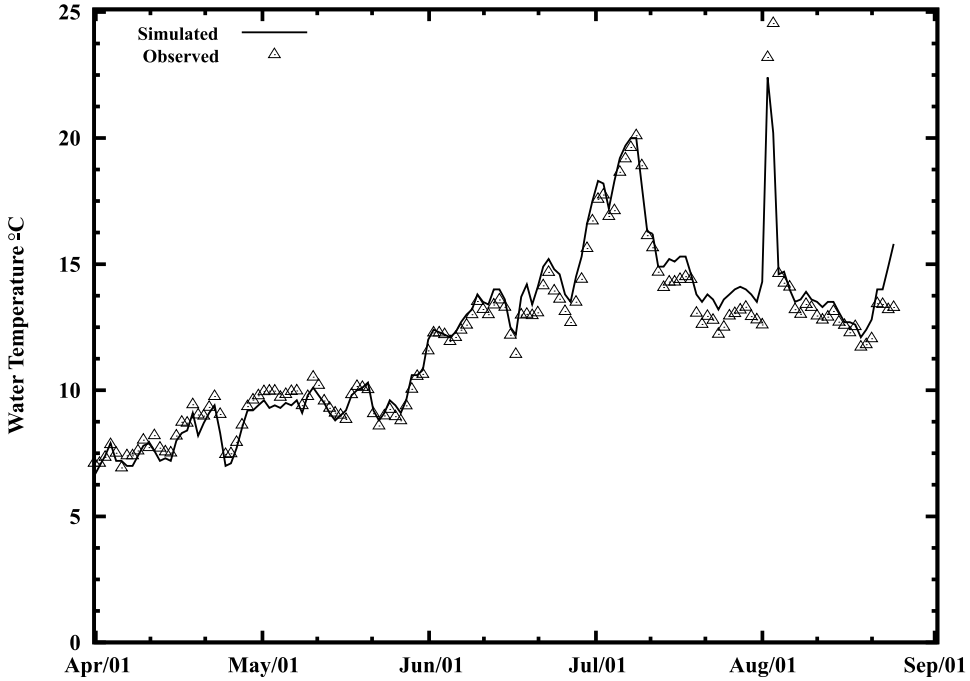

Figure 7. Simulated and observed daily average water temperatures in the Clearwater River at Lewiston, Idaho, 1998.

Figures 7 and 8. Average and standard deviation of the differences between daily averaged and hourly predicted and observed temperatures are shown in Table 3.

4.3. Columbia River, Washington and Oregon

[38] The Columbia River system drains more than 670,800 km^2 of southeastern British Columbia in Canada and parts of the states of Idaho, Oregon, Washington and Wyoming. The main stem Columbia River enters the United States in northeastern Washington (Figure 9) and flows 1200 km to the Pacific Ocean near Astoria, Oregon. Its annual average streamflow at its mouth is 6540 m^3/s. The Columbia River and its major tributaries, the Snake and Willamette rivers have been developed to a high degree by

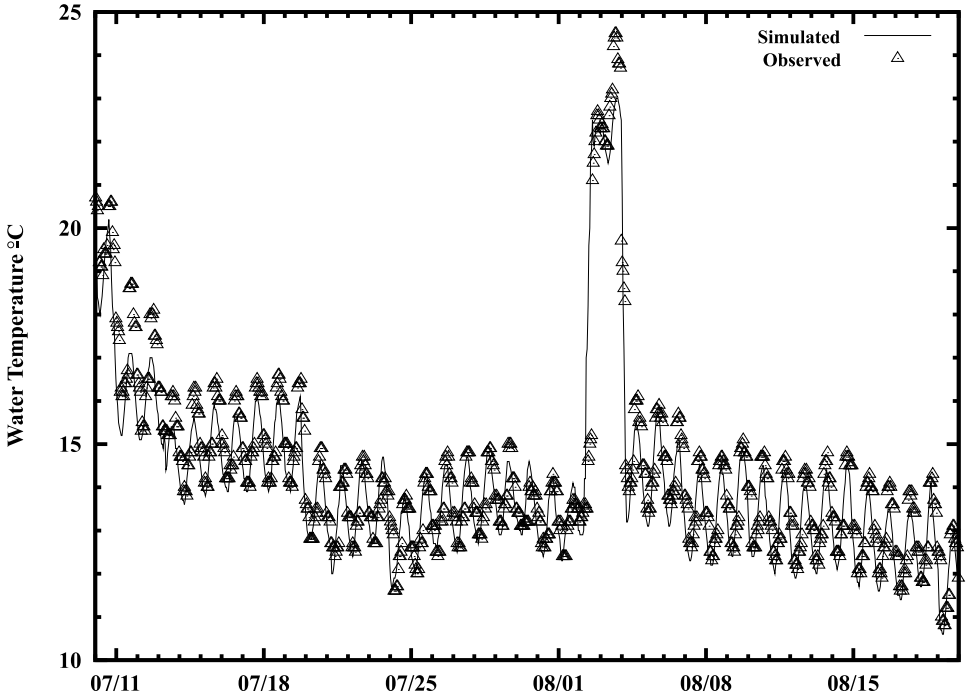

Figure 8. Simulated and observed hourly water temperatures in the Clearwater River at Spalding, Idaho, July–August 1998.

Table 3. Mean and Standard Deviation of Differences Between Simulated and Observed Temperatures in the Columbia and Snake Rivers

River System	Location	Time Period	Mean	Standard Deviation
Columbia	Grand Coulee Dam	1995–1999	0.03	0.96
Columbia	Bonneville Dam	1995–1999	−0.42	0.95
Clearwater	Lewiston, Idaho	1998 daily average	−0.31	0.67
Clearwater	Spalding, Idaho	1998 hourly	−0.63	0.61
Snake	Ice Harbor Dam	1995–1999	−0.10	0.97

dams and reservoirs that are operated for multiple purposes, including irrigation, navigation, flood control, municipal and industrial water supply, recreation and hydroelectric power generation. Development of the Columbia River system has resulted in important changes to the water temperature regime [*Yearsley et al.*, 2001]. As a result, many segments of the Columbia River system fail to meet water temperature criteria established to protect cold water biota (Washington Department of Ecology, Washington State's Water Quality Assessment, 2009, available at http://www.ecy.wa.gov/programs/wq/303d/index.html).

[39] Section 303 d(2) of the Federal Clean Water Act requires that a TMDL be prepared. Application of the energy budget method has proven to be a valuable tool in drafting a TMDL for water temperature in the segments of the Columbia and Snake rivers in Idaho, Oregon and Washington that fail to meet water quality standards [*Yearsley*, 2003b]. The model application described here formed the basis for drafting the TMDL and is an example of model performance at large time and space scales.

[40] Other than a 102 km segment below Priest Rapids Dam, the segments of the Columbia and Snake rivers included in this study (Figure 9) are characterized by a series of reservoirs associated with hydroelectric projects. Lake Roosevelt, the reservoir created by Grand Coulee Dam is the only project in the study area that is operated for flood control and for which there are significant changes in reservoir elevation. With the exception of Lake Roosevelt on the Columbia River and Lower Granite on the Snake River, the dams in the study segment are vertically well mixed. Lake Roosevelt is a deep reservoir with depths exceeding 100 m. However, it is only a weakly stratified reservoir due to the high flow in the Columbia River [*Yearsley*, 2003a]. Significant stratification in the reservoir behind Lower Granite occurs when there are density flows resulting from releases of cold water at Dworshak Dam on the Clearwater River.

[41] Testing of the semi-Lagrangian method in the Columbia and Snake River segments with the water temperature model RBM10 was performed using water temperature and flow data from continuous monitors at dam sites, archived on the DART data site and available at http://www.cbr.washington.edu/dart/. Observed flows from the DART site were used to estimate river speeds for the RBM10 model. Hydraulic properties of the river and reservoir segments were made available by the USACE Portland District office. Depth and velocity as a function of time and space for freely flowing segments were estimated with relationships of the form given by (16) and (17). Depth and velocity as a function of time and space in reservoirs were estimated from the continuity equation. Meteorological data from the National Climatic Data Center (NCDC) Surface Airways weather stations shown in Table 4 was used to compute the exchange of energy across the air-water interface, $H_{air\text{-}water}$.

[42] The geographical scope of the simulations (Figure 9) included the Snake River from below Lewiston, Idaho (Snake River kilometer 270.4), the Clearwater River near Dworshak Dam (Clearwater River kilometer 64.4), the Columbia River at the International Boundary between Canada and the United States (Columbia River kilometer 1199) and Bonneville Dam (river kilometer 235.0), the most

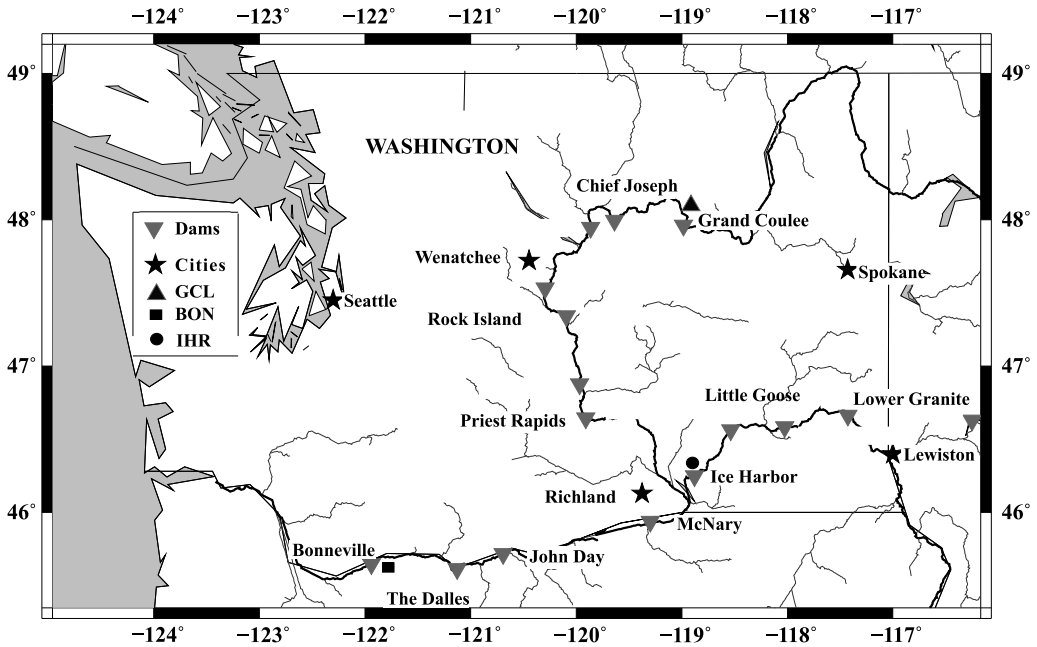

Figure 9. Columbia and Snake river system in Idaho, Oregon, and Washington.

Table 4. Location of Weather Stations Used to Estimate Energy Budget for the Columbia and Snake River Water Temperature Simulations

River System	River Segment (km)	River Location	WBAN Station Number	WBAN Station Location
Clearwater	67.6–0.0	Dworshak Dam–Lewiston	24149	Lewiston, Idaho
Snake	270.4–119.4	Lewiston, Idaho–Little Goose Dam	24149	Lewiston, Idaho
Snake	119.4–0.0	Little Goose Dam–Ice Harbor Dam	24243	Yakima, Washington
Columbia	1188.0–960.1	International Boundary–Grand Coulee Dam	24127	Spokane, Washington
Columbia	960.1–729.7	Grand Coulee Dam–Rock Island Dam	94239	Wenatchee, Washington
Columbia	729.7–234.2	Rock Island Dam–Bonneville Dam	24243	Yakima, Washington

downstream project on the Columbia River. Bonneville Dam is where tidal influence of the Pacific Ocean is observed. For these tests, the simulations were terminated in the forebay of Bonneville Dam. Ice Harbor Dam on the Snake River is near the confluence of the Columbia and Snake rivers. Simulated and observed temperatures at these locations on the Columbia and Snake rivers are shown in Figures 10–12.

4.4. Application to Impacts of Climate Change

[43] Climate change is an environmental issue with potential impacts across a broad spectrum of space and time. *Meyer et al.* [1999], for example, discuss many aspects of the effects of climate change on the health of aquatic ecosystems and describe potential ecological risks that are complex ecologically and, by implication, complex spatially and temporally. There is concern in regions like the Pacific Northwest and Alaska where habitat for cold water species, particularly salmonids, may be at risk from increased temperatures.

[44] Given the highly scalable nature of the semi-Lagrangian method, it has considerable potential for developing an understanding of climate change impacts on aquatic ecosystems. A preliminary investigation of its utility for addressing the impact climate change on water temperature was conducted with the Columbia River basin in Idaho, Oregon and Washington (Figure 9) as a prototype.

[45] In the Columbia River system, cold water species are important components of aquatic ecosystems. Many populations of salmonids in this region are at risk or endangered [*Independent Scientific Group*, 1996]. As part of an ongoing study of climatic impacts on water resources in the Pacific Northwest for the University of Washington Climate Impacts Group, the Variable Infiltration Capacity (VIC) [*Liang et al.*, 1994; *Nijssen and Lettenmaier*, 1997] macroscale hydrology model was linked with the GENESYS (available at http://www.nwcouncil.org/energy/genesys/about.htm) hydroelectric and thermal power generation model of the Pacific Northwest Power and Conservation Council; and the semi-Lagrangian water temperature model

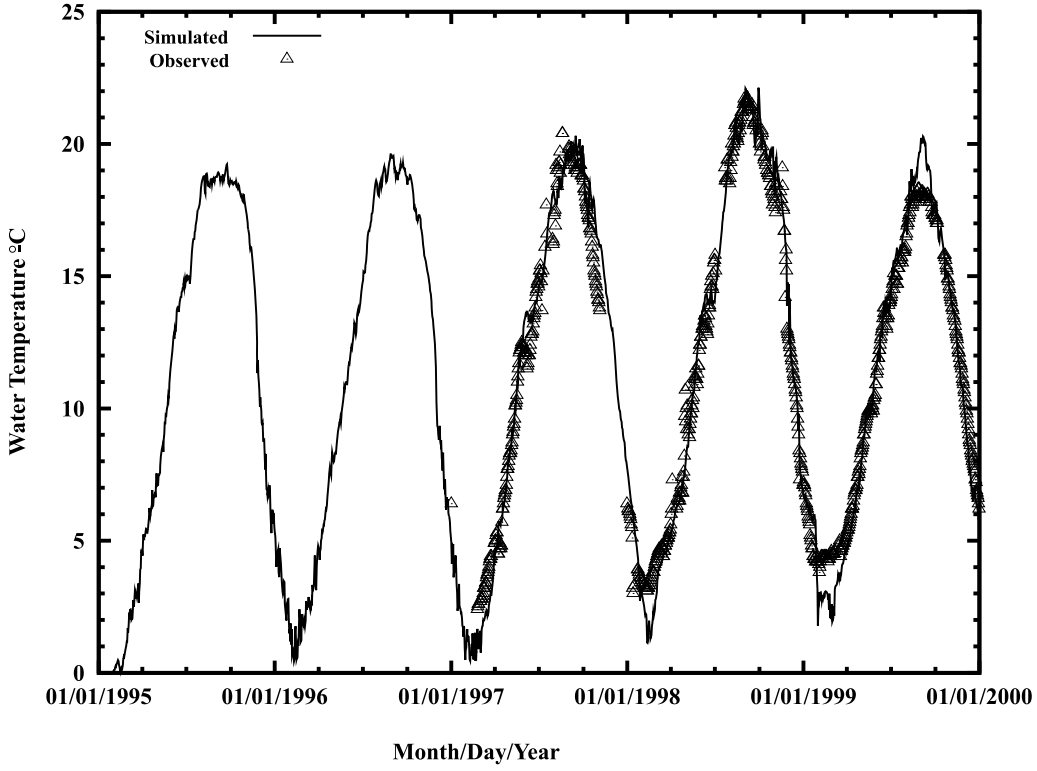

Figure 10. Simulated and observed water temperatures in the Columbia River below Grand Coulee Dam, 1995–2000.

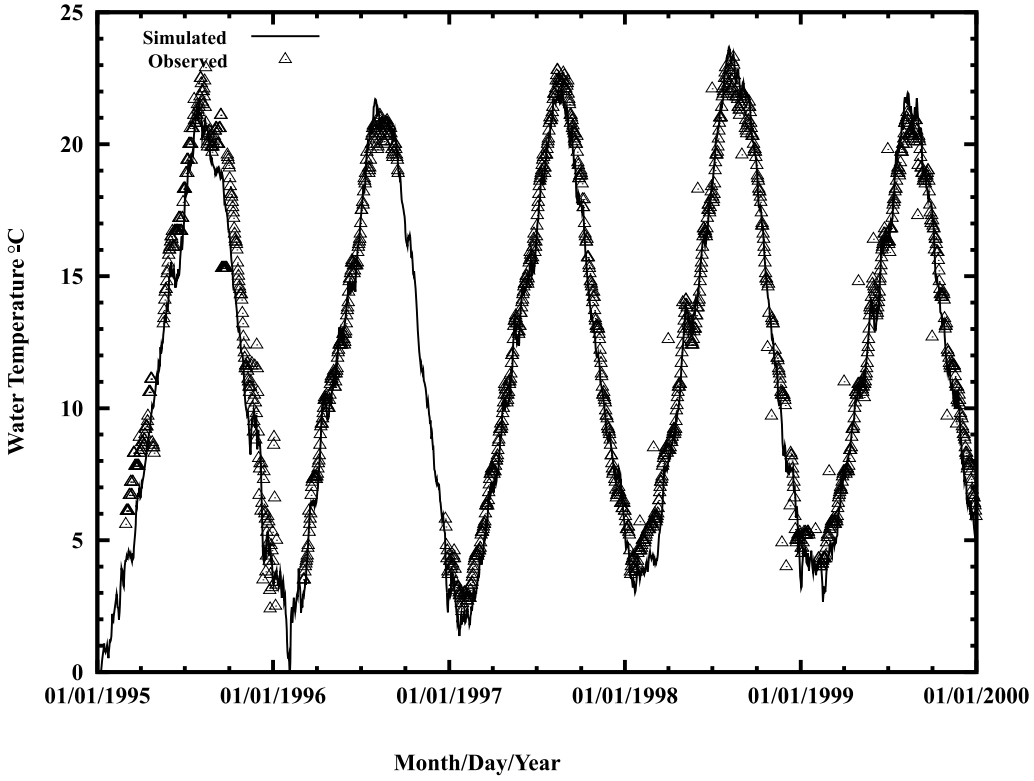

Figure 11. Simulated and observed water temperatures in the Columbia River in the forebay of Bonneville Dam, 1995–2000.

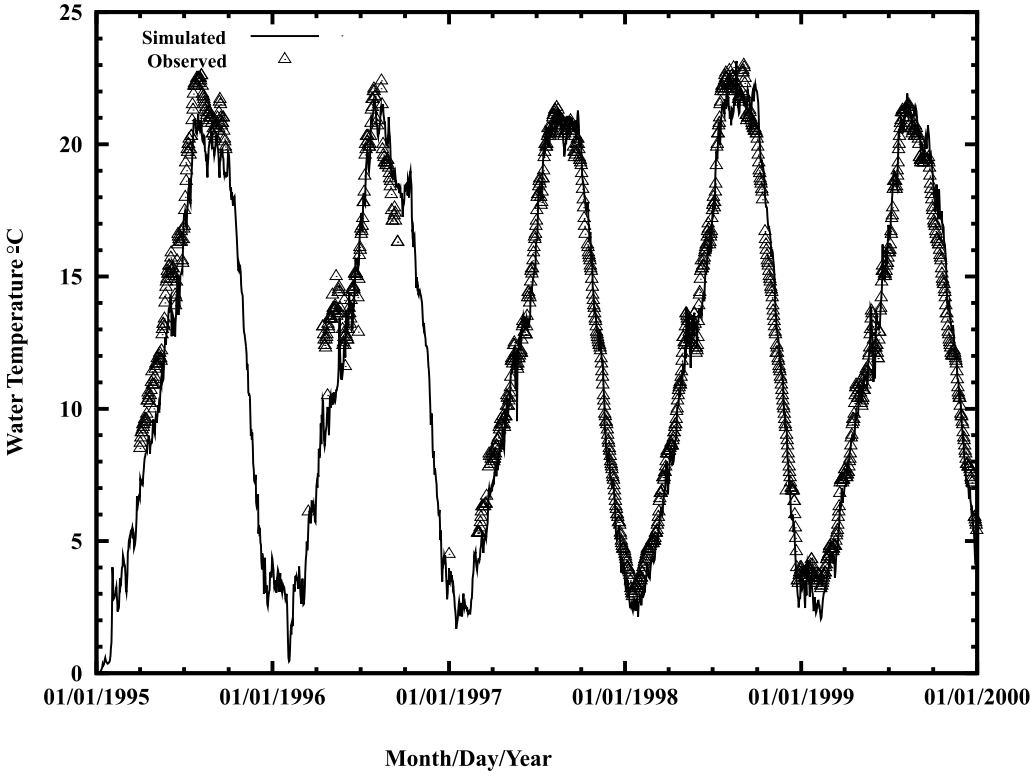

Figure 12. Simulated and observed water temperatures in the Snake River below Ice Harbor Dam, 1995–2000.

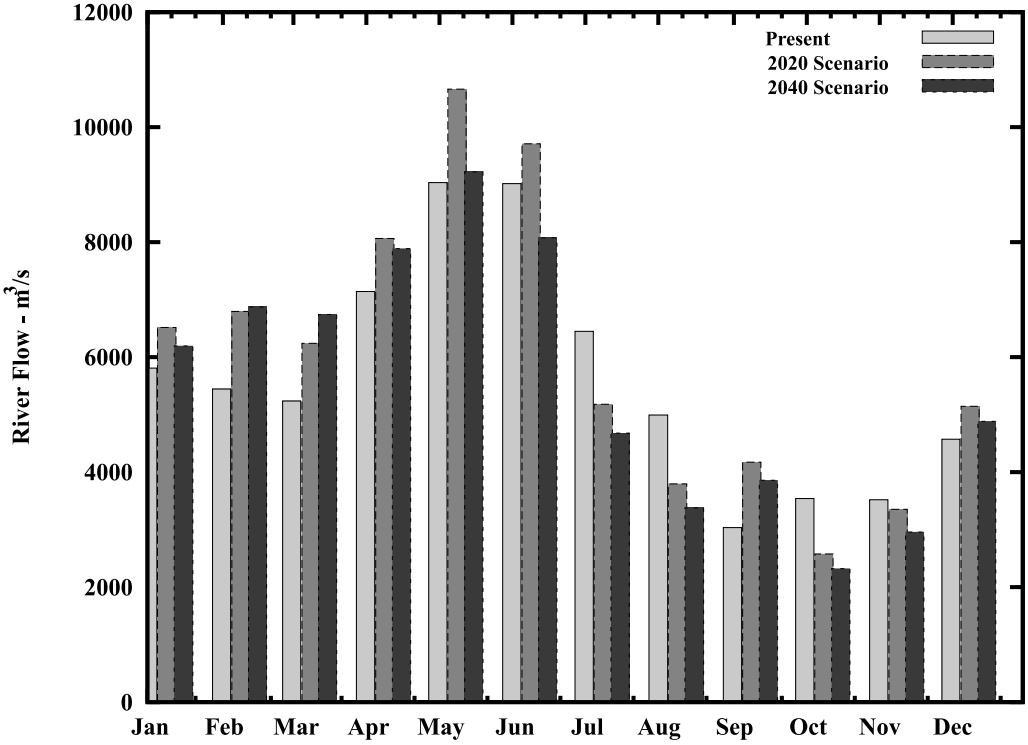

Figure 13. Simulated monthly average flow in the Columbia River at Bonneville Dam for three climate scenarios (present climate, 2020, and 2040).

to simulate the effects of climate change on water temperatures in Snake and Columbia River reservoirs. The domain of the water temperature study included the main stem Columbia River from the U.S.-Canadian border to Bonneville Dam, as well as the Snake River from near Lewiston, Idaho to its confluence with the Columbia River and 24 major tributaries.

[46] The VIC hydrologic model was run using a gridded climatological data set described by *Maurer et al.* [2002] adjusted by mean (monthly) temperature and precipitation changes from the output of four global General Circulation Models (GCMs) for years 2020 and 2040. The global climate models used for these scenarios were the U.K. Met Office Hadley Centre Climate models, HadCM2 and HadCM3, the Max Planck Institute model, ECHAM4, and the Department of Energy model, PCM3 [*Snover et al.*, 2003]. "Present climate" was described as the average of weather conditions for 1951–1978. Results were downscaled using the "delta" method described by *Hamlet and Lettenmaier* [1999] and *Snover et al.* [2003].

[47] VIC simulates the "natural" hydrology. Comparison of simulations using VIC and observed natural flows is described, for example, in the work of *Hamlet and Lettenmaier* [1999]. However, the Columbia River system is highly regulated for flood control and power generation and the level of development changed during the period 1951–1978 as more hydroelectric projects were constructed. To account for the effects of regulation and to normalize the operation based on the present state of development, the results from VIC were processed with the GENESYS model. Rule curves employed by the GENESYS model were based on hydrology data from the Columbia River system for the period 1951–1978. Average monthly flows for this period of record, as processed by the GENSYS model, were generated using the present climate conditions (1951–1978) and the composite of the climate results for 2020 and 2040 from the four GCMs. The monthly averaged flows for the Columbia River at Bonneville Dam (Columbia River kilometer 235.0) and the Snake River at Ice Harbor Dam (Snake River kilometer 16.0) are shown in Figures 13 and 14.

[48] The hydrologic results from the process described were used in conjunction with the climate data from the A1B scenario produced under the auspices of the Intergovernmental Panel on Climate Change [*IPCC*, 2000] as input to the water temperature model. A 28-year time series of daily averaged water temperatures was simulated using these hydrologic and climatological data.

[49] Average daily temperatures for the 28-year simulations for each of the three climate scenarios (present climate, 2020, 2040) are shown for two locations, Bonneville Dam on the Columbia River and Ice Harbor Dam on the Snake River (Figures 15 and 16). The simulated average increases in water temperature at these locations compared to present climate for the two climate change scenarios, 2020 and 2040 are shown in Figures 17 and 18.

5. Discussion

[50] The nominal solution for the linearized form of a one-dimensional water temperature model with state space structure has been developed using a semi-Lagrangian numerical scheme and the energy budget method as the deterministic input. Incorporating this solution into (8) and (9) for estimating water temperatures and its uncertainty

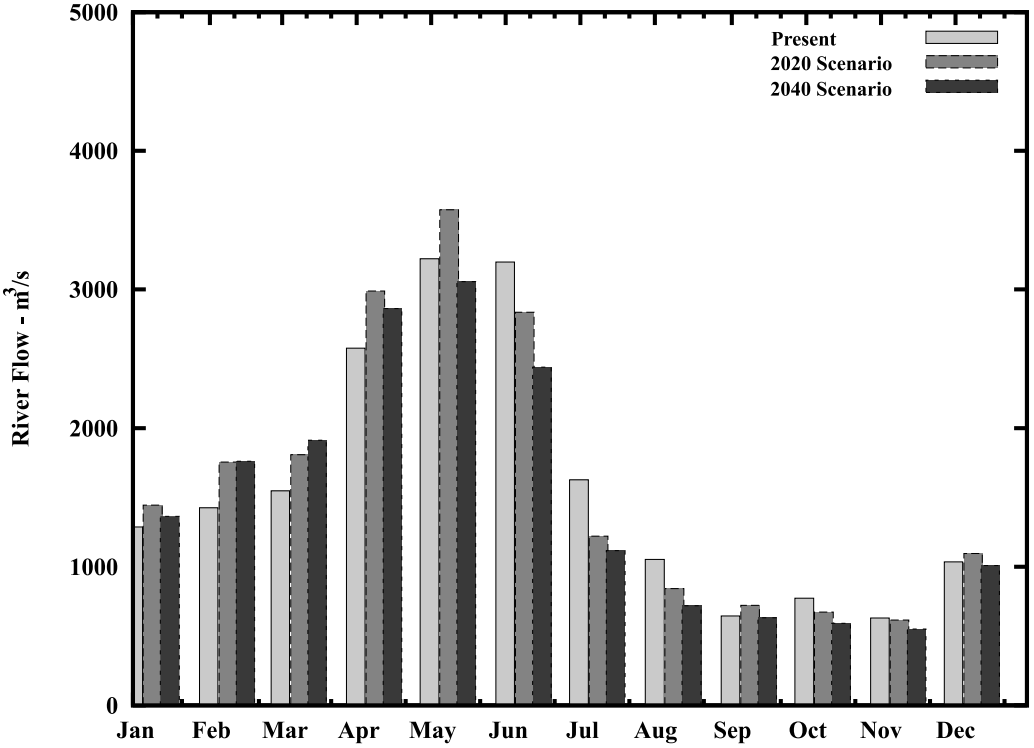

Figure 14. Simulated monthly average flow in the Snake River at Ice Harbor Dam for three climate scenarios (present climate, 2020, and 2040).

depends on how well it satisfies the key assumption of small differences between the nominal and true state.

[51] In the tests comparing simulated results with the analytical solution when$0.5 \leq T_{res} \leq 1$, the semi-Lagrangian numerical method shows no numerical dispersion when the residence time, T_{res}, is an integer. Numerical dispersion becomes more of an issue for SRPT when the residence time is not an integer or when the size of the finite difference

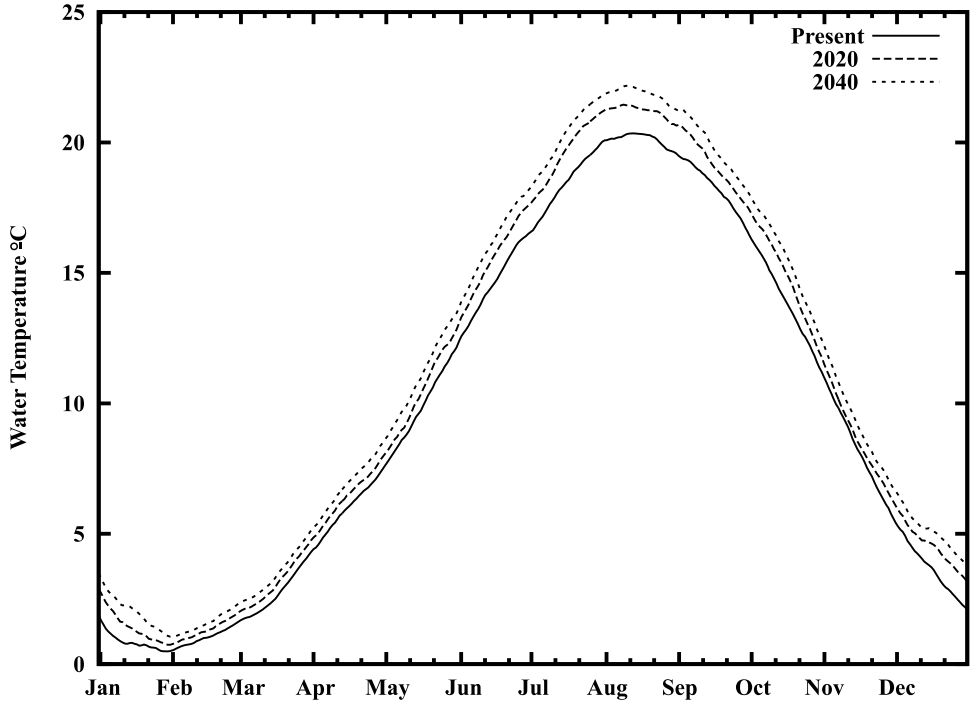

Figure 15. Simulated daily average water temperature in the Columbia River at Bonneville Dam for three climate scenarios (present climate, 2020, and 2040).

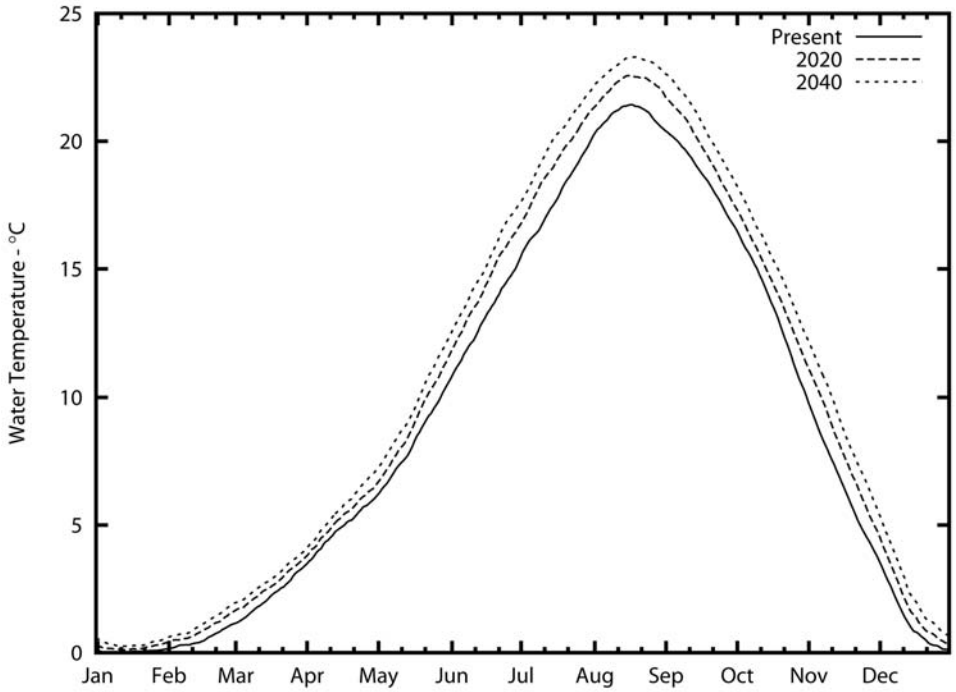

Figure 16. Simulated daily average water temperatures in the Snake River at Ice Harbor Dam for three climate scenarios (present climate, 2020, and 2040).

segments is not all equal [*Yearsley et al.*, 2001]. Although these tests were limited to $N_{Cr} \leq 2$, *Manson et al.* [2001] used similar numerical examples to evaluate the computational efficiency and accuracy of their semi-Lagrangian method, DISCUS, for $N_{Cr} \leq 50$. In their examples, accuracy and efficiency of the semi-Lagrangian method increased as the Courant number, N_{Cr}, increased.

[52] The accuracy of the reverse particle tracking semi-Lagrangian method used in this work does, however, decrease noticeably when the residence time is greater than

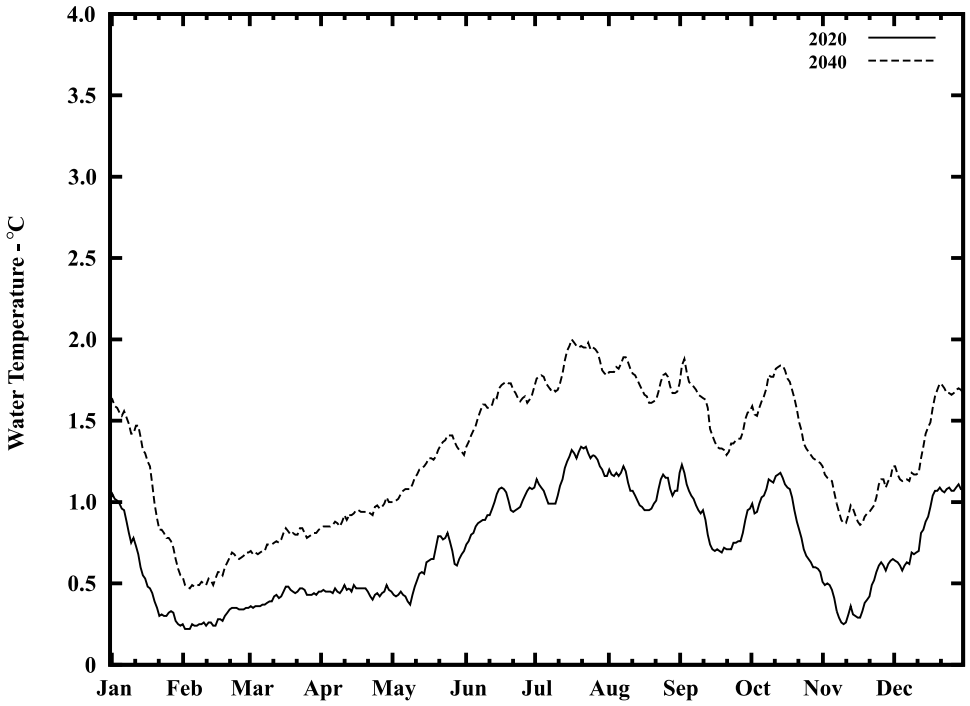

Figure 17. Simulated increase in daily average water temperature in the Columbia River at Bonneville Dam compared to present climate for two climate scenarios (2020 and 2040).

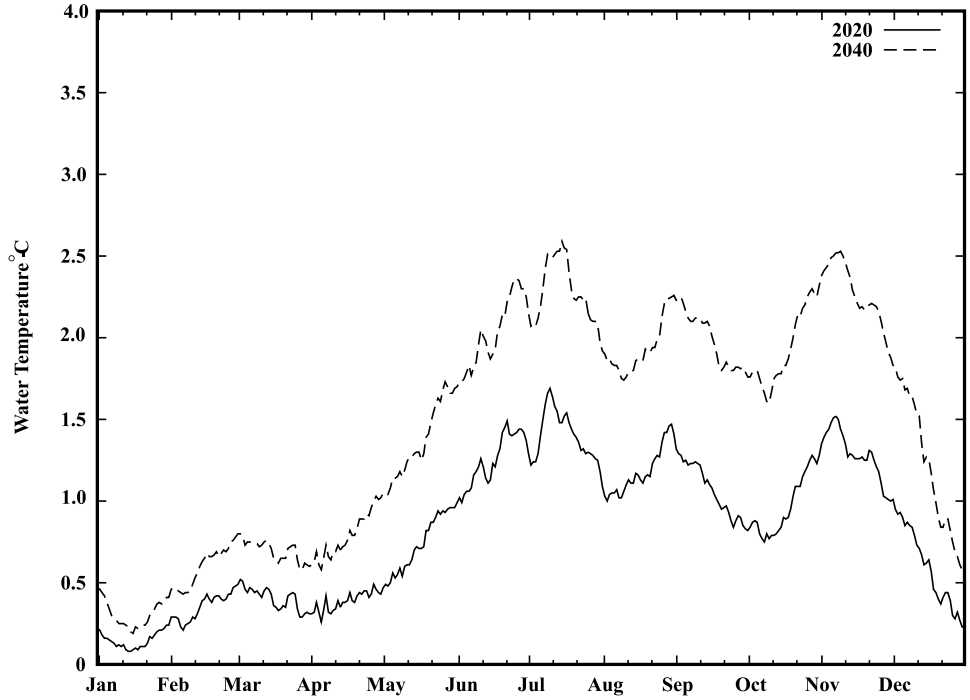

Figure 18. Simulated increase in daily average water temperature in the Snake River at Ice Harbor dam compared to present climate for two climate scenarios (2020 and 2040).

one unless the segment length is decreased sufficiently. Decreasing the segment length, Δx_j, so as to increase the Courant number, N_{Cr}, is equivalent in terms of computational efficiency to decreasing the time step for explicit Eulerian schemes like QUICK. Furthermore, as *Manson et al.* [2001] point out there is a computational burden associated with the semi-Lagrangian method in performing the interpolation. The net result being there may be little computational advantage to using semi-Lagrangian methods for $N_{Cr} < 1$, particularly when higher-order interpolation schemes are used. In the case of the applications described above, third-order polynomial interpolation was used. At the cost of decreasing accuracy simulating sharp fronts, the computational burden can be reduced by using lower order polynomials. Although not tested here, it may make sense to do this in river systems for which longitudinal variations in water temperature are small.

[53] The tests comparing simulated results with the known solutions of the numerical example focus on the accuracy of the semi-Lagrangian numerical method and its capability for reproducing sharp concentration fronts when advection dominates. Although these examples are in no way exhaustive, they do agree with the findings of others [e.g., *Cheng et al.*, 1984; *Manson et al.*, 2001] regarding the ability of semi-Lagrangian method to minimize or eliminate numerical dispersion. Additional examples of the performance of the numerical scheme described here can be found in the work of *Yearsley et al.* [2001]. The findings described here for the analytical solutions are supported in the case of natural systems by the results obtained in the study of the Clearwater River (section 4.2).

[54] The applications to the natural river systems described in sections 4.2 and 4.3 provide a means for evaluating the robustness of the energy budget and the degree to which the model is appropriate for the nominal solution in (8) and (9) for real systems.

[55] In the examples taken from the Clearwater and Columbia river systems, estimates of the true state are based on measurements of water temperature using measurement devices with some degree of uncertainty. In addition, the temperature measurements from the above examples are all at a single point in the river and must be mapped to the cross-sectionally averaged temperature simulated by the model. In the above examples the mapping is one to one. That is, the observed point temperature was assumed to be equal to the cross-sectionally averaged temperature. With the understanding that the observations are only an estimate of the true system state, they are used here to estimate statistics of the difference between the nominal (simulated) system state and the "true" state.

[56] Standard deviations of the difference between simulated and observed (Table 3) for the simulations of the Clearwater River, Snake River and Columbia are similar to the results obtained in the application of the thermal energy budget method to the river systems mentioned previously (Table 1). In the case of the Columbia and Snake river simulations, differences between predicted and observed are due primarily to what can be characterized as parameter estimation rather than to the inaccuracies in the numerical scheme. Uncertainty in parameter estimation includes weather data from distant locations to characterize heat fluxes, estimating hydraulic variables using simplified stream hydrodynamics, and uncertainty in the formulation of energy budget terms.

[57] The numerical scheme plays a more important role in the Clearwater River simulations because of the sharp concentration front and the higher frequencies (daily) in the thermal energy budget. Based on the statistics for the

differences between simulated and observed (Table 3), as well as comparison with the results from other studies, the semi-Lagrangian method gives results within the limits of accuracy imposed by uncertainty in parameters. Although the primary motivation for the development of the semi-Lagrangian method is for applications to large-scale systems, the results from the Clearwater River demonstrate the applicability of the method to smaller systems with high frequency inputs.

[58] Research in progress at the University of Washington, NOAA's Northwest Fisheries Science Center and the National Center for Ecological Analysis and Synthesis (NCEAS) in Santa Barbara, California focuses on the response of salmon to climate change in the rivers of California, Oregon, Washington, British Columbia and Alaska. The scope of this and similar projects is several orders of magnitude larger than that of the preliminary analysis of section 4.4 or of studies described above in the Columbia River [*Richmond and Perkins*, 2002] and Fraser River [*Morrison et al.*, 2002]. Water temperature is a critical component of aquatic ecosystem habitat and applications of the energy budget method at this scale will require significant computational resources. The robustness, computational efficiency and accuracy of the semi-Lagrangian method described here make it well suited for large-scale applications of this type.

[59] The linearization methods described for propagating variance (8) and (9) can also be applied to the development of recursive filters [*Schweppe*, 1973; *Gelb et al.*, 1974]. Recursive filters are used in data assimilation methods in oceanography, meteorology and hydrology for state estimation; parameter estimation; the design of monitoring networks; and forecasting. Potential applications of data assimilation to water temperature are suggested by the growing need in the Pacific Northwest to maintain habitat for salmonids. The semi-Lagrangian model, RBM10, is used as a decision support tool to forecast and manage flow and water temperature releases from Dworshak Dam on the North Fork of the Clearwater River in Idaho (Figure 5). Although this example is not one requiring significant computing resources, it is not difficult to envision similar efforts of greater size; efforts that will benefit from application of state estimation methods and computationally efficient, accurate numerical methods.

6. Conclusions

[60] This paper describes a computationally efficient, accurate numerical scheme for modeling water temperature in advection-dominated streams, rivers and reservoirs. The numerical scheme exploits the virtues of a Lagrangian frame of reference for computational efficiency and accuracy; and tracks simulated results on a fixed grid that is a feature of Eulerian solution techniques. The model is developed as the nominal solution within state space structure within which estimates of water temperature are treated as random variables.

[61] Computational efficiency and accuracy of the nominal solution are demonstrated by comparison of model estimates with observations of stream temperatures from rivers in the Pacific Northwest as well as with results from a closed-form solution of the energy equation. A preliminary analysis of the impact of climate changes on stream temperature in the Columbia River system illustrates the strengths of the semi-Lagrangian method for addressing water quality issues of regional, national and, ultimately, global scale. Further development of the semi-Lagrangian method has the potential to improve the ability of water quality planners to perform uncertainty analysis, risk analysis and forecasting for large, complex river systems.

[62] **Acknowledgments.** I would like to thank Dennis Lettenmaier for his review of drafts of this paper and for his many helpful suggestions. Marketa McGuire Elsner and Alan Hamlet provided the forcing function data for the various climate change scenarios. I would also like to thank Elizabeth Clark for her assistance preparing the graphics. This publication is (partially) funded by the Joint Institute for the Study of the Atmosphere and Ocean (JISAO) under NOAA Cooperative Agreement NA17RJ1232, contribution 1779.

References

Boyd, M., and B. Kasper (2003), Analytical methods for dynamic open channel heat and mass transfer: Methodology for heat source model version 7.0, Oreg. Dep. of Environ. Qual., Portland.

Brown, L. C., and T. O. Barnwell Jr. (1987), The enhanced stream water quality models QUAL2E and QUAL2E-UNCAS, *Rep. EPA/600/3-87/007*, Environ. Resour. Lab., U.S. Environ. Prot. Agency, Athens, Ga.

Burkholder, B. K., G. E. Grant, R. Haggerty, T. Khangaonkar, and P. J. Wampler (2008), Influence of hyporheic flow and geomorphology on temperature of a large, gravel-bed river, Clackamas River, Oregon, USA, *Hydrol. Processes*, *22*, 941–953, doi:10.1002/hyp.6984.

Burt, W. V. (1958), Heat budget terms for Middle Snake River Reservoir, in *Water Temperature Studies on the Snake River*, *Tech. Rep. 6*, U.S. Fish and Wildlife Serv., Washington, D. C.

Chapra, S. C. (1997), *Surface Water-Quality Modeling*, McGraw-Hill, New York.

Chapra, S. C., G. J. Pelletier, and H. Tao (2008), QUAL2K: A modeling framework for simulating river and stream water quality, version 2.11: Documentation and users manual, Civ. and Environ. Eng. Dep., Tufts Univ., Medford, Ma.

Cheng, R. T., V. Casulli, and S. N. Milford (1984), Eulerian-Lagrangian solution of the convection-dispersion equation in natural coordinates, *Water Resour. Res.*, *20*(7), 944–952, doi:10.1029/WR020i007p00944.

Cole, T. M., and S. A. Wells (2002), CE-QUAL-W2: A two-dimensional, laterally averaged, hydrodynamic and water quality model, version 3.1, *Instr. Rep. EL-02-1*, U.S. Army Corps of Eng., Vicksburg, Miss.

Collins, W. D., P. J. Rasch, B. A. Boville, J. J. Hack, J. R. McCaa, D. S. L. Williamson, J. T. Kiehl, and B. B. Briegleb (2004), Description of the NCAR Community Atmosphere Model (CAM 3.0), *Tech. Note NCAR/TN-464+STR*, Clim. and Global Dyn. Div., Natl. Cent. for Atmos. Res., Boulder, Colo.

Delay, W. H., and J. Seaders (1966), Predicting temperature in rivers and reservoirs, *J. Sanit. Eng. Div.*, *92*, 115–134.

Donato, M. M. (2002), A statistical model for estimating stream temperatures in the Salmon and Clearwater River basins, central Idaho, *U.S. Geol. Surv. Water Resour. Invest. Rep., 02-4195*.

European Centre for Medium-Range Weather Forecasts (2006), IFS documentation Cy31r1, operational implementation, part III: Dynamics and numerical procedures, Reading, U. K.

Edinger, J. E., D. K. Brady, and J. C. Geyer (1974), Heat exchange and transport in the environment, *Rep. 14*, Electr. Power Resour. Inst., Palo Alto, Calif.

Foreman, M. G. G., C. B. James, M. C. Quick, P. Hollemans, and E. Wiebe (1997), Flow and temperature models for the Fraser and Thompson rivers, *Atmos. Ocean*, *35*(1), 109–134.

Foreman, M. G. G., D. K. Lee, J. Morrison, S. Macdonald, D. Barnes, and I. V. Williams (2001), Simulations and retrospective analyses of Fraser watershed flows and temperatures, *Atmos. Ocean*, *39*(2), 89–105.

Gelb, A., J. F. Kasper Jr., R. A. Nash Jr., C. F. Price, and A. A. Sutherland Jr. (1974), *Applied Optimal Estimation*, MIT Press, Cambridge, Mass.

Hamlet, A. F., and D. P. Lettenmaier (1999), Effects of climate change on hydrology and water resources in the Columbia River basin, *J. Am. Water Res. Assoc.*, *35*(6), 1597–1623, doi:10.1111/j.1752-1688.1999.tb04240.x.

Hydrologic Engineering Center (2002), HEC-RAS: River analysis system, version 3.0, U.S. Army Corps of Eng., Davis, Calif.

Independent Scientific Group (1996), *Return to the River: Restoration of Salmonid Fishes in the Columbia River Ecosystem*, Northwest Power Plann. Counc., Portland, Oreg.

Intergovernmental Panel on Climate Change (2000), *Special Report on Emissions Scenarios. A Special Report of Working Group III of the Intergovernmental Panel on Climate Change*, edited by N. Nakicenovic and R. Swart, Cambridge Univ. Press, Cambridge, U. K.

Intergovernmental Panel on Climate Change (2007), Summary for policymakers, in *Climate Change 2007: Impacts, Adaptation and Vulnerability. Contribution of Working Group II to the Fourth Assessment Report of the Intergovernmental Panel on Climate Change*, edited by M. L. Parry et al., pp. 7–22, Cambridge Univ. Press, Cambridge, U. K.

Jobson, H. E. (1981), Temperature and solute-transport simulation in streamflow using a Lagrangian reference frame, *U.S. Geol. Survey Water Resour. Invest. Rep., 81-2*.

Jobson, H. E., and D. H. Schoellhamer (1993), Users manual for a branched Lagrangian transport model, *U.S. Geol. Survey Water Resour. Invest., 87-4163*.

King, I. P. (1996a), RMA-11; a two-dimensional finite element model for water quality, version 2.1, Resour. Manage. Assoc., Suisun, Calif.

King, I. P. (1996b), RMA-2; a two-dimensional finite element model for flow in estuaries and streams, version 5.1, Resour. Manage. Assoc., Suisun, Calif.

Leonard, B. P. (1979), A stable and accurate convective modeling procedure based on quadratic upstream interpolation, *Comput. Methods Appl. Mech. Eng.*, *19*, 59–98, doi:10.1016/0045-7825(79)90034-3.

Leonard, B. P. (1991), The ULTIMATE conservative difference scheme applied to unsteady one-dimensional advection, *Comput. Methods Appl. Mech. Eng.*, *88*, 17–74, doi:10.1016/0045-7825(91)90232-U.

Leopold, L. B., and T. Maddock (1953), The hydraulic geometry of channels and some physiographic implications, *U.S. Geol. Surv. Prof. Pap.*, 252.

Liang, X., D. P. Lettenmaier, E. F. Wood, and S. J. Burges (1994), A simple hydrologically based model of land surface water energy fluxes for general circulation models, *J. Geophys. Res.*, *99*(D7), 14,415–14,428, doi:10.1029/94JD00483.

Manson, J. R., and S. G. Wallis (2000), A conservative, semi-Lagrangian fate and transport model for fluvial systems—I. Theoretical development, *Water Res.*, *34*(15), 3769–3777, doi:10.1016/S0043-1354(00)00131-7.

Manson, J. R., S. G. Wallis, and D. Hope (2001), A conservative semi-Lagrangian transport model for rivers with transient storage zones, *Water Resour. Res.*, *37*(12), 3321–3329, doi:10.1029/2001WR000230.

Maurer, E. P., A. W. Wood, J. C. Adam, D. P. Lettenmaier, and B. Nijssen (2002), A long-term hydrologically based data set of land surface fluxes and states for the conterminous United States, *J. Clim.*, *15*, 3237–3251, doi:10.1175/1520-0442(2002)015<3237:ALTHBD>2.0.CO;2.

Meyer, J. L., M. J. Sale, P. J. Mulholland, and N. L. Poff (1999), Impacts of climate change on aquatic ecosystem functioning and health, *J. Am. Water Resour. Assoc.*, *35*, 1373–1386, doi:10.1111/j.1752-1688.1999.tb04222.x.

Mohseni, O., H. G. Stefan, and T. R. Erickson (1998), A nonlinear regression model for weekly stream temperatures, *Water Resour. Res.*, *34*(10), 2685–2693, doi:10.1029/98WR01877.

Morrison, J., M. C. Quick, and M. G. G. Foreman (2002), Climate change in the Fraser River watershed: Flow and temperature projection, *J. Hydrol.*, *263*(1–4), 230–244, doi:10.1016/S0022-1694(02)00065-3.

Nijssen, B., and D. P. Lettenmaier (1997), Streamflow simulation for continental-scale river basins, *Water Resour. Res.*, *33*(4), 711–724, doi:10.1029/96WR03517.

Pan, M., and E. F. Wood (2006), Data assimilation for estimating the terrestrial water budget using a constrained ensemble Kalman filter, *J. Hydrometeorol.*, *7*(3), 534–547, doi:10.1175/JHM495.1.

Poole, G. C., and C. H. Berman (2001), An ecological perspective on in-stream temperature: Natural heat dynamics and mechanisms of human caused degradation, *Environ. Manage. N. Y.*, *27*, 787–802, doi:10.1007/s002670010188.

Press, W. H., B. P. Flannery, S. A. Teukolsky, and W. T. Vetterling (1986), *Numerical Recipes: The Art of Scientific Computing*, Cambridge Univ. Press, New York.

Raphael, J. M. (1962), Prediction of temperature in rivers and reservoirs, *J. Power Div. Am. Soc. Civ. Eng.*, *2*, 157–181.

Richmond, M. C., and W. A. Perkins (2002), Regional scale simulation of water temperatures variations in the Columbia River basin, paper presented at Research and Extension Regional Water Quality Conference, Coop. State Res., Educ., and Ext. Serv., U.S. Dep. of Agric., Vancouver, Wash., February.

Richmond, M., W. Perkins, and Y. Chien (2000), Numerical model analysis of systemwide dissolved gas abatement alternatives, *Contract DACW68–96-D-0002*, Battelle Pac. Northwest Div., Richland, Wash.

Risley, J. C., E. A. Roehl Jr., and P. A. Conrads (2003), Estimating water temperatures in small streams in Western Oregon using neural networks, *U.S. Geol. Survey Water Resour. Invest. Rep., 02-4218*.

Roache, P. J. (1976), *Computational Fluid Dynamics*, Hermosa, Albuquerque, N. M.

Schweppe, F. C. (1973), *Uncertain Dynamic Systems*, Prentice-Hall, Englewood Cliffs, N. J.

Sinokrot, B. A., and H. G. Stefan (1993), Stream temperature dynamics: Measurements and modeling, *Water Resour. Res.*, *29*(7), 2299–2312, doi:10.1029/93WR00540.

Snover, A. K., A. F. Hamlet, and D. P. Lettenmaier (2003), Climate change scenarios for water planning studies, *Bull. Am. Meteorol. Soc.*, *84*(11), 1513–1518.

Sridhar, V., A. L. Sansone, J. Lamarche, T. Dubin, and D. P. Lettenmaier (2004), Prediction of stream temperature in forested watersheds, *J. Am. Water Res. Assoc.*, *40*(1), 197–213, doi:10.1111/j.1752-1688.2004.tb01019.x.

Stow, C. A., and D. Scavia (2009), Modeling hypoxia in the Chesapeake Bay: ensemble estimation using a Bayesian hierarchical model, *J. Mar. Syst.*, *76*, 244–250, doi:10.1016/j.jmarsys.2008.05.008.

Sullivan, A. B., and S. A. Rounds (2004), Modeling streamflow and water temperature in the North Santiam and Santiam rivers, Oregon, 2001–02, *U.S. Geol. Survey Water Resour. Invest. Rep., 2004-5001*, 35 pp.

Sverdrup, H. U., M. W. Johnson, and R. H. Fleming (1942), *The Oceans, Their Physics, Chemistry, and General Biology*, Prentice-Hall, New York.

Theurer, F. D., K. A. Voos, and W. J. Miller (1984), Instream water temperature model, *Instream Flow Inf. Pap. 16*, U.S. Fish and Wildlife Serv., Fort Collins, Colo.

Toprak, Z. F., and M. E. Savci (2007), Longitudinal dispersion coefficient modeling in natural channels using fuzzy logic, *Clean Soil Air Water*, *35*(6), 626–637.

Vrugt, J. A., H. V. Gupta, B. O. Nuallain, and W. Bouten (2006), Real-time data assimilation for operational ensemble streamflow forecasting, *J. Hydrometeorol.*, *7*, 548–565, doi:10.1175/JHM504.1.

Wunderlich, W. O., and R. Gras (1967), Heat and mass transfer between a water surface and the atmosphere, Div. of Water Pollut. Control Plann., Tenn. Valley Authority, Norris.

Yearsley, J. R. (2003a), Columbia River temperature assessment: Simulation of the thermal regime of Lake Roosevelt, *Rep. EPA 910-C-03-00*, U.S. Environ. Prot. Agency, Seattle, Wash.

Yearsley, J. R. (2003b), Developing a temperature TMDL for the Columbia and Snake rivers: Simulation methods, *Rep. EPA-910-R-03-003*, U.S. Environ. Prot. Agency, Seattle, Wash.

Yearsley, J., D. Karna, S. Peene, and B. Watson (2001), Application of a 1-D heat budget model to the Columbia River system, *Rep. EPA 910-R-01-004*, U.S. Environ. Prot. Agency, Seattle, Wash.

Yeh, G. T. (1990), A Lagrangian-Eulerian method with zoomable hidden fine-mesh approach to solving advection-dispersion equations, *Water Resour. Res.*, *26*(6), 1133–1144.

Zhang, R., K. Huang, and M. T. van Genuchten (1993), An efficient Eulerian-Lagrangian method for solving solute transport problems in steady and transient flow fields, *Water Resour. Res.*, *29*(12), 4131–4138, doi:10.1029/93WR01674.

J. R. Yearsley, Department of Civil Engineering, University of Washington, Box 352700, Seattle, WA 98195, USA. (yearsley@hydro.washington.edu)